

Jamming by shape in kinetically constrained models

Eial Teomy* and Yair Shokef†

School of Mechanical Engineering, Tel Aviv University, Tel Aviv 69978, Israel

(Received 16 January 2014; published 14 March 2014)

We derive expressions for the critical density for jamming in a hyper-rhomboid system of arbitrary shape in any dimension for the Kob-Andersen and Fredrickson-Andersen kinetically constrained models. We find that changing the system's shape without altering its total volume or particle density may induce jamming. We also find a transition between shapes in which the correlation length between jammed particles is infinite and shapes that have a finite correlation length.

DOI: [10.1103/PhysRevE.89.032204](https://doi.org/10.1103/PhysRevE.89.032204)

PACS number(s): 45.70.-n, 64.60.an, 64.70.Q-

I. INTRODUCTION

Increasing the density of particles in granular materials causes them to undergo a transition from an unjammed state, in which the particles can move relatively freely, to a jammed state, in which almost none of the particles can move [1–4]. Systems of interest in nature and in industrial applications typically have complicated geometries which strongly affect jamming in them [5–8], and it is thus important to understand how confinement influences the jamming of granular matter. Here we investigate the effects of confinement on the jamming transition, and in particular test how the shape of containers, and not only their volume, determines how they jam. Most theoretical work so far was done on square and cubic systems, or even in the infinite system size limit [9–14].

There are numerous laboratory experiments that deal with nonsquare two-dimensional systems [15–18]. For example, Daniels and Behringer conducted an experiment on polypropylene spheres in an annulus [19], which is large enough to be considered a rectangle with infinite length and finite width. A different experiment by Bi *et al.* [20] consists of shearing a square system such that it becomes a rectangle with the same area and particle density as the original square. Other experiments, such as [21–24], considered colloids confined between quasiparallel plates.

In this paper we examine the effects of confinement on jamming by studying these phenomena in kinetically constrained models in d -dimensional hyper-rhomboids. The essence of jamming is captured by the various kinetically constrained models [25–42]. Such simple models, and other related models [43–54], have exact solutions, which help us to obtain deep insights into the physical processes responsible for the corresponding phenomena in real systems.

A. Models

We consider the Kob-Andersen (KA) [55] and Fredrickson-Andersen (FA) [56,57] models on hypercubic lattices of arbitrary dimension d . The system is confined to a hyper-rhombus of size $L_1 \times \dots \times L_d$, such that $L_i \leq L_{i+1}$ for all $1 \leq i \leq d-1$. In the KA model each site may be occupied by at most one particle, and a particle can move to a neighboring

vacant site if it has at least m neighboring vacancies before and after the move. In the FA model a site can change its state from occupied to vacant or vice versa if it has at least m neighboring vacancies. If $m = 1$, then even a single vacancy can facilitate the movement of the entire system, and thus all the particles can move eventually regardless of the system's shape or size. If m is less than or equal to the system's dimension d , there are no frozen particles in an infinite system. However, if at least $d - m + 1$ of the system's sides are of finite size, there is a finite probability that there will be a frozen structure spanning the system from one edge to the other. If m is larger than the system's dimension, consider a completely occupied d -dimensional small hypercube inside the system. Each particle in this hypercube has at most d neighboring vacancies and so will never move. Hence, there is always a finite fraction of frozen particles even for an infinite system. Moreover, these frozen particles are not necessarily connected to the system's edges and can be “free floating” in the middle, and we do not refer to this situation as jammed. In general, there is a finite probability for having frozen particles as long as at least $d - m + 1$ of the rhomboid's sides are finite.

For infinite systems, the critical density is the density at which the fraction of frozen particles is singular [31–33]. Although no real phase transition occurs in finite systems, there is a crossover transition between an almost unfrozen regime, in which almost all of the particles on average are unfrozen, to a frozen regime, in which almost all the particles are frozen. We use the average fraction of frozen particles, n_F , as the order parameter, and define the critical density as the density at which on average half of the particles are frozen, $n_F = 1/2$. With hard-wall boundary conditions, our order parameter can be thought of as a point-to-set correlation function [58,59], because it measures the probability that a particle is frozen given that the outside edges of the system are blocked.

Balogh *et al.* showed that for the FA model in a hypercube with $L_i = L$, the critical vacancy density is [60]

$$v_{d,m} = \left(\frac{\lambda_{d,m}}{\ln_{(m-1)} L} \right)^{d-m+1}, \quad (1)$$

where $\ln_{(k)}(x) = \ln\{\ln[\dots \ln(x) \dots]\}$ is the ln function iterated k times,

$$\lambda_{d,m} = \int_0^\infty g_{m-1}(z^{d-m+1}) dz, \quad (2)$$

*eialteom@post.tau.ac.il

†shokef@tau.ac.il

and

$$g_k(z) = -\ln \left[\frac{1 - e^{-kz} + \sqrt{(1 + e^{-kz})^2 - 4e^{-(k+1)z}}}{2} \right]. \quad (3)$$

In particular, for $d = 2$, the only nontrivial case is $m = 2$, for which

$$\begin{aligned} v_{2,2} &= \frac{\lambda_{2,2}}{\ln L}, \\ \lambda_{2,2} &= \frac{\pi^2}{18} \approx 0.5483 \dots, \end{aligned} \quad (4)$$

and for $d = 3$, both $m = 2$ and $m = 3$ are nontrivial, with

$$\begin{aligned} v_{3,2} &= \left(\frac{\lambda_{3,2}}{\ln L} \right)^2, & v_{3,3} &= \frac{\lambda_{3,3}}{\ln \ln L} \\ \lambda_{3,2} &= 0.9924 \dots, & \lambda_{3,3} &= 0.4039 \dots \end{aligned} \quad (5)$$

This is correct only asymptotically for very large systems. For finite systems, there is some effective value of $\lambda_{d,m}$ which converges to these values for extremely large L [61]. In what follows, whenever $\lambda_{d,m}$ appears, it should be understood as this effective $\lambda_{d,m}$.

Although for $m \leq d$ the critical vacancy density in the thermodynamic limit ($L \rightarrow \infty$) is $v_c = 0$, it is still important to know the effects that the size and shape of the system have on v_c , since real and simulated systems are of finite size and can be of different shapes. It is also interesting to investigate systems which are infinite or very large in some directions and finite or small in other directions, such as very long tunnels that have a finite width. In [62] we investigated two-dimensional rectangular systems in the $m = 2$ FA and KA models, and found that the critical vacancy density in infinitely long tunnels with a finite width W scales as $v_{2,2} \propto \frac{1}{\sqrt{W}}$, which is qualitatively different from $v_c \propto 1/\ln L$ for square systems in Eq. (4). Here, we expand our previous work by considering d -dimensional hyper-rhomboids with any $1 < m \leq d$.

B. Outline

In this work we distinguish between weak confinement and strong confinement, depending on the number of effective dimensions of the hyper-rhomboid, d_{eff} . A tunnel, for example, has one effective dimension, $d_{\text{eff}} = 1$, while a three-dimensional (3D) system confined between closely separated parallel walls has $d_{\text{eff}} = 2$. Consider a system in which d_{eff} of its sides are infinite, and the other $s = d - d_{\text{eff}}$ sides are finite. If $d_{\text{eff}} \geq m$, then none of the particles in the system are frozen, while if $d_{\text{eff}} < m$ a finite fraction of the particles is frozen. When the system is of finite size, its critical density is mainly governed by the size of the largest d_{eff} dimensions if $d_{\text{eff}} \geq m$, or by the size of the smallest s dimensions if $d_{\text{eff}} < m$. Hence, we define a weakly confined system as a system with $d_{\text{eff}} \geq m$ (since the confinement in the s small dimensions has only a weak effect), and a strongly confined system as a system with $d_{\text{eff}} < m$.

A weakly confined system is characterized by long-range correlations. By making a small, local change in the configuration, the entire system can change from being unjammed to jammed and vice versa. In a strongly confined system,

the correlations are short ranged. There are clusters of frozen and unfrozen particles, such that a small local change in the configuration may change the state of the local cluster, but not of the entire system.

We also find analytical expressions for the critical density for different hyper-rhomboids. By changing the system's shape, but not its total volume or particle density, the critical density also changes, such that it may be above the particle density for some shape but below it for a different shape. Hence, a system may jam and/or unjam by changing only its shape.

The remainder of this article is organized as follows. In Sec. II we analyze the critical densities for hyper-rhomboids. We present here a derivation of the critical density for three-dimensional systems, and reserve the derivation for general dimensions for Appendix C. In Sec. III we show how changing the shape of a system induces jamming by studying the $m = 2$ model in three-dimensional rhomboids. In Sec. IV we study the correlation between frozen sites in strongly confined three-dimensional systems in the $m = 3$ model. Section V summarizes our work.

II. CRITICAL DENSITY

In this section we show the derivation of the critical density for d -dimensional rhomboids in any $m \leq d$. We first present a sketch of the derivation, and later show the full details. Those not interested in the more technical details can read only the beginning of this section and skip the subsections. A detailed derivation of the critical density for general dimensions appears in Appendix C.

Consider first a special case of weakly confined systems, namely, hypercubes. The system is unfrozen if it contains at least one critical droplet, which is a small unblocked region that can cause the entire system to become unblocked [63]. We denote the probability that a site is part of a critical droplet which unblocks a hypercube of size L^d by $P[L \times \dots \times L]$. The average number of sites which seed a critical droplet is thus $L^d P[L \times \dots \times L]$. The system is unfrozen when it contains at least one critical droplet. Therefore, the critical density is found by solving the equation

$$1 = L^d P[L \times \dots \times L]. \quad (6)$$

Holroyd [63] showed that for two-dimensional systems with $m = 2$ the probability of seeding a droplet is

$$P[L \times L] = \exp[-2\lambda_{2,2}/(1 - \rho)], \quad (7)$$

where $\lambda_{2,2}$ is given in Eq. (4) above. Thus Eq. (1) is retrieved for the two-dimensional square with $m = 2$. Balogh *et al.* [60] used the same idea for d -dimensional hypercubes in any $m \leq d$ to derive Eq. (1) for hypercubes in any dimension.

The main idea is to start from a very small unblocked region and try to expand it isotropically in all directions by checking if the sites adjacent to the unblocked region satisfy some condition (which depends on d and m). Therefore, the most probable shape that a droplet can unblock is a hypercube. However, other shapes, as long as they are not too deformed, can also be unblocked by a single droplet, because the system's edges do not impede the expansion of the droplet. We show below (for $d = 3$) and in Appendix C

(for $d > 3$) that for weakly confined systems ($d_{\text{eff}} \geq m$), if there is a critical droplet, it will unblock the entire system with high probability. The implication of this is that if a particle is frozen, there is no critical droplet, and thus the other particles in the system are highly likely to be frozen as well. Hence, the correlation between frozen particles spans the entire system, no matter its size. By calculating the probability that a particle in a hyper-rhomboid is part of a critical droplet, $P[L_1 \times \dots \times L_d]$, and solving the analog to Eq. (6):

$$1 = VP[L_1 \times \dots \times L_d], \quad (8)$$

where V is the volume of the system, we find the critical vacancy density

$$v_c^{\text{weak}} = \frac{1}{V_s} \left(\frac{\lambda_{d_{\text{eff}},m}}{\ln_{(m-1)} V^{1/d_{\text{eff}}}} \right)^{d_{\text{eff}}-m+1}, \quad (9)$$

where $s = d - d_{\text{eff}}$ and

$$V_s = \prod_{i=1}^s L_i \quad (10)$$

is the volume associated with the small dimensions. Except for the prefactor of $1/V_s$, the critical density is the same as for a hypercube with d_{eff} dimensions. Note that for weakly confined systems the critical density depends on the ratios between the lengths L_i only via the number of effective dimensions. This means that as long as the hyper-rhomboid is not too deformed, its critical density is equal to the critical density of a hypercube of equal volume.

As will be explained in Secs. II A and II B, due to the way the droplet is constructed and expanded, it needs at least m dimensions in order to expand indefinitely. Therefore, in a strongly confined system ($d_{\text{eff}} < m$), the system's edges block the expansion of the critical droplet, and thus each droplet unblocks only part of the system. These unfrozen clusters have a characteristic size ξ , and we assume that at the critical density the frozen and unfrozen clusters have the same characteristic size. The critical density is found by evaluating the density at which half of the clusters contain a droplet, i.e., by solving the equation

$$\frac{1}{2} = V_{\text{cluster}} P[\text{cluster}], \quad (11)$$

where V_{cluster} is the volume of a typical cluster and $P[\text{cluster}]$ is the probability that a site will seed a critical droplet that unblocks the cluster. The solution to this equation is

$$v_c^{\text{strong}} \sim \left[\ln_{(m-2)} V_s^{1/(d-t)} \right]^{-d+t+m-1}, \quad (12)$$

where t is the number of very small dimensions (for example, a 3D system with $L_3 \gg L_2 \gg L_1$ has $s = 2$ and $t = 1$), and $\ln_{(0)} x \equiv x$. This expression is similar to the critical density of a weakly confined system with $d - t - 1$ dimensions in an $m - 1$ model. In effect, the strong confinement removes one degree of freedom.

It is important to note that the value of the parameter λ given in Eq. (2) is valid only for very large systems. For $m = 2$ in $d = 2$ it is well known that even for the largest systems that have been simulated ($L \approx 10^5$) $\lambda_{2,2}$ is equal to roughly half of its asymptotic value [61,64]. By considering other ways to

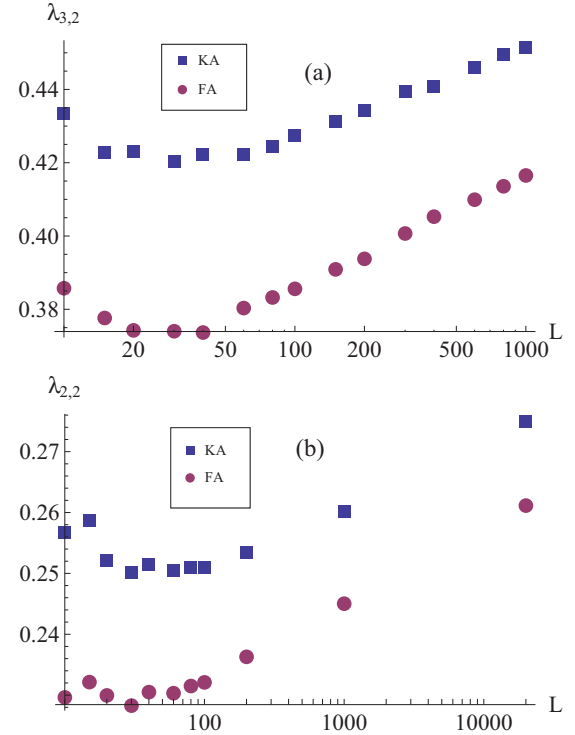


FIG. 1. (Color online) The effective values of $\lambda_{3,2} = \sqrt{v_c} \ln L$ for cubes of size L^3 (a) and of $\lambda_{2,2} = v_c \ln L$ for squares of size L^2 (b) in the KA (blue squares) and the FA (red circles) models. The values of λ in the sizes sampled are far from their asymptotic values of $\lambda_{3,2} \approx 0.99$ and $\lambda_{2,2} \approx 0.54$, and they appear to behave as $\sim \ln L$.

expand the droplet, Gravner and Holroyd [61] evaluated the asymptotic corrections to this value, and estimated that systems as large as $L = 10^{20}$ would be needed to observe convergence in the numerical value of $\lambda_{2,2}$. Here we see a similar behavior for $d = 3$.

Figure 1 shows the effective value of $\lambda_{3,2} = \sqrt{v_c} \ln L$ in cubes of size L^3 and of $\lambda_{2,2} = v_c \ln L$ in squares of size L^2 . Under our current computational limits ($L^d \leq 10^9$, which requires 30 Gbytes of memory), the effective $\lambda_{3,2}$ has a value of approximately 0.45 in the KA model and 0.42 in the FA model, far from its asymptotic value of ≈ 0.99 . However, it is clear that it grows with L . Theoretically, the value of λ for both models should be the same. The added constraint in the KA model reduces the probability of unblocking the entire system, and thus increases λ , and this effect is non-negligible in small systems. Figure 2 shows the critical vacancy density and the effective $\lambda_{3,3}$ for cubes of different sizes in the $m = 3$ model. Similarly to the $m = 2$ model, the effective λ is far from its asymptotic value of 0.4.

In order to find the critical densities numerically, we first calculated the fraction of frozen particles, n_F , for many densities. The critical density was estimated by a linear interpolation between the two densities for which n_F was the closest to 0.5. For each density, n_F was calculated as an average over several thousands of random configurations, such that the relative error in the critical vacancy density $\delta v_c/v_c$ is 1% or lower.

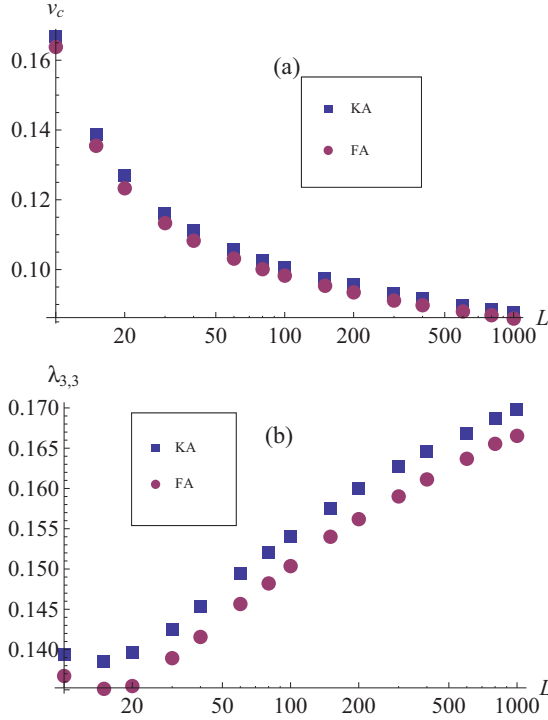


FIG. 2. (Color online) The critical vacancy density v_c (a) and the effective $\lambda_{3,3} = v_c \ln \ln L$ (b) for three-dimensional cubes as a function of the cube size L in the $m = 3$ model. The effective $\lambda_{3,3}$ is far from its asymptotic value of 0.4.

A. Derivation of the critical density for the $m = 2$ model

In this section we first sketch the derivation of Eq. (1) given in [60] for hypercubes in arbitrary dimensions for the $m = 2$ model. For simplicity we give it here for three dimensions. The generalization to higher dimensions is straightforward. We will then consider three-dimensional rhomboids.

1. Cubes

When $m = 2$, a cube ($L_1 = L_2 = L_3 \equiv L$) is either completely unfrozen or almost completely frozen. The system can become unfrozen if it contains at least one critical droplet. We denote the probability that a site is part of a critical droplet which unblocks a system of size $L \times L \times L$ by $P[L \times L \times L]$. The average number of sites which seed a critical droplet is thus $L^3 P[L \times L \times L]$. The system is unfrozen when it contains at least one critical droplet. Therefore, the critical density is found by solving the equation

$$1 = L^3 P[L \times L \times L]. \quad (13)$$

In order for a site to be in a critical droplet, we first consider a small $2 \times 2 \times 2$ cube and randomly choose one of the eight $3 \times 3 \times 3$ cubes that contain it. We then check whether this $3 \times 3 \times 3$ cube is frozen or not. We want to continue this process to a $4 \times 4 \times 4$ cube and so on until the entire system is unfrozen. The original $2 \times 2 \times 2$ cube is a critical droplet only if it is possible to expand it to the system's size. Assume that we now want to check whether a box of size $(l + 1) \times (l + 1) \times (l + 1)$ is frozen or not. The probability that it is not frozen is $P[(l + 1) \times (l + 1) \times (l + 1)]$. We start from a cube

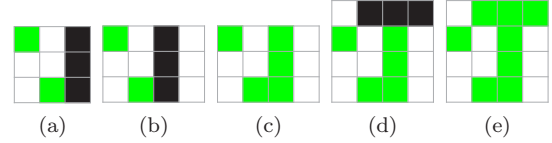


FIG. 3. (Color online) An example of the expansion of a critical droplet in $d = 2$. We start from panel (a) with a 3×3 system. The particles shown in green (gray) are unfrozen, and the black particles are those that either are blocked at that stage of the expansion or are newly considered. Now, expand it to the right (b). The rightmost column is not full, and the 3×2 rectangle is unfrozen. This means that the 3×3 square satisfies the second condition, and the 3×4 rectangle is unfrozen (c). We now expand it one row upwards (d). The top row is not full, which means that the first condition is satisfied, and thus the entire 4×4 square is unfrozen (e).

of size $l \times l \times l$ and expand it in three steps: first to a rhomboid of size $l \times l \times (l + 1)$, then to $l \times (l + 1) \times (l + 1)$, and lastly to $(l + 1) \times (l + 1) \times (l + 1)$. In the first step, the rhomboid is unblocked if one of two disjoint conditions occur: either the $l \times l \times l$ box is unblocked and the added side is not full, or the $l \times l \times (l - 1)$ rhomboid is unblocked, the sites in the side of the $l \times l \times l$ box but not in the $l \times l \times (l - 1)$ rhomboid are all occupied, and the added side of the $l \times l \times (l + 1)$ rhomboid is not full. See Fig. 3 for an illustration of the expansion process in two dimensions. Hence $P[l \times l \times (l + 1)]$ satisfies the equation

$$P[l \times l \times (l + 1)] = P[l \times l \times l](1 - \rho^{l^2}) + P[l \times l \times (l - 1)]\rho^{l^2}(1 - \rho^{l^2}), \quad (14)$$

where ρ is the particle density.

The assumption that these probabilities have the form

$$P[l_1 \times l_2 \times l_3] = \prod_{l=1}^{l_1} \beta(l^2) \prod_{l=1}^{l_2} \beta(l^2) \prod_{l=1}^{l_3} \beta(l^2) \quad (15)$$

yields

$$P[l \times l \times (l + 1)] = P[l \times l \times (l - 1)]\beta[(l + 1)^2]\beta(l^2) \quad (16)$$

and

$$P[l \times l \times l] = P[l \times l \times (l - 1)]\beta(l^2). \quad (17)$$

Using this assumption in Eq. (14) yields

$$\beta[(l + 1)^2]\beta(l^2) = (\beta(l^2) + \rho^{l^2})(1 - \rho^{l^2}). \quad (18)$$

Further assuming that for large l , β depends weakly on it, namely, $\beta[(l + 1)^2] \approx \beta(l^2)$ in Eq. (18), we have a quadratic equation for β with the solution

$$\beta(l^2) = \frac{1 - \rho^{l^2} + \sqrt{1 + 2\rho^{l^2} - 3\rho^{2l^2}}}{2}. \quad (19)$$

The other two steps of the rhomboid expansion yield similar equations for β . By assuming that β depends weakly on l for large l , the solution of these two equations is the same as in Eq. (19).

Therefore, the probability that a certain site is part of a critical droplet, i.e., that it can unblock the entire system, is

$$P[L \times L \times L] = \left[\prod_{l=1}^L \beta(l^2) \right]^3 = \exp \left[3 \sum_{l=1}^L \ln \beta(l^2) \right]. \quad (20)$$

Since the critical density in an infinite system is 1 and the critical density in finite systems is close to 1 we can approximate ρ^{l^2} by

$$\rho^{l^2} \approx \exp[-vl^2], \quad (21)$$

where $v = 1 - \rho$ is the vacancy density. For large enough L ($L \geq 10$), the value of the probability $P[L \times L \times L]$, calculated via Eq. (20), is very close to the probability of expanding the droplet to infinity, $P[\infty \times \infty \times \infty]$ as shown in Fig. 4, so we can use the latter even for finite systems.

Changing the summation in Eq. (20) to an integration over $z = \sqrt{v}l$ yields according to the Euler-Maclaurin formula

$$\begin{aligned} P[\infty \times \infty \times \infty] &\approx \exp \left\{ 3 \int_{\sqrt{v}}^{\infty} \ln \left[\beta \left(\frac{z^2}{v} \right) \right] \frac{dz}{\sqrt{v}} + \frac{3}{2} [\ln \beta(\infty) + \ln \beta(1)] \right\} \\ &= \exp \left\{ 3 \int_{\sqrt{v}}^{\infty} \ln \left[\beta \left(\frac{z^2}{v} \right) \right] \frac{dz}{\sqrt{v}} + \frac{3}{2} \ln \beta(1) \right\}. \end{aligned} \quad (22)$$

Taking the limit $v \ll 1$ yields

$$P[\infty \times \infty \times \infty] = \exp \left\{ -\frac{3[\lambda_{3,2} + \sqrt{v}(\frac{\ln v}{4} - 1)]}{\sqrt{v}} \right\}, \quad (23)$$

where

$$\begin{aligned} \lambda_{3,2} &= - \int_0^{\infty} \ln \left(\frac{1 - e^{-z^2} + \sqrt{1 + 2e^{-z^2} - 3e^{-2z^2}}}{2} \right) dz \\ &\approx 0.9924. \end{aligned} \quad (24)$$

Using this result in Eq. (13) yields Eq. (2). The transition from the sum to the integral is valid for very small v and large L as shown in Fig. 4.

2. Three-dimensional rhomboids: Weak confinement

We now assume that the three length scales $L_1 \leq L_2 \leq L_3$ are not necessarily equal. We repeat the derivation of the critical droplets, such that the critical density is found from the relation

$$1 = L_1 L_2 L_3 P[L_1 \times L_2 \times L_3]. \quad (25)$$

We assume that the form of P is

$$P[L_1 \times L_2 \times L_3] = \prod_{l=1}^{L_1} \beta^3(l^2) \prod_{l=L_1+1}^{L_2} \beta^2(L_1 l) \prod_{l=L_2+1}^{L_3} \beta(L_1 L_2). \quad (26)$$

The derivation of the expansion of the critical droplets is the same as in cubes until $l = L_1$. At that point, we can expand the rhomboid in only two directions and the size of the third side is fixed to be L_1 . Then, when $l = L_2$, we can expand in only one direction and the sizes of the other two sides are L_1 and L_2 .

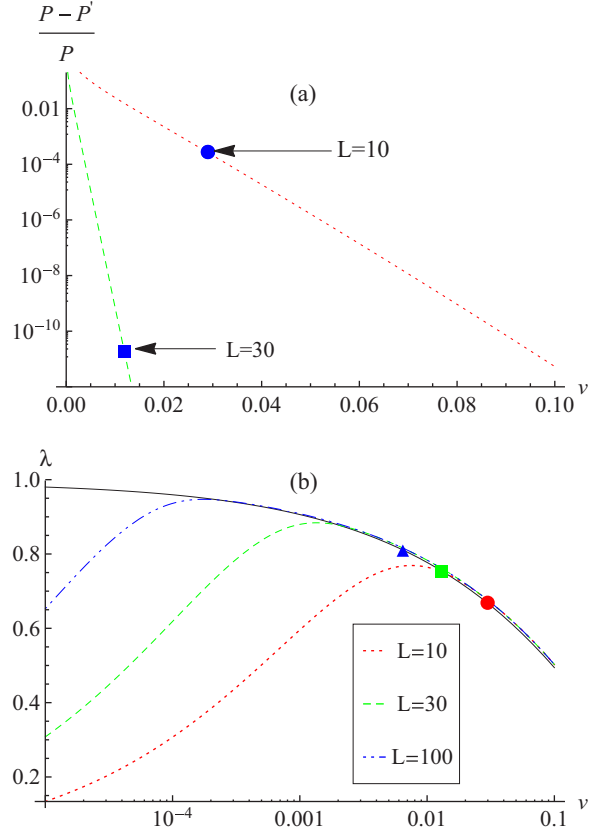


FIG. 4. (Color online) (a) The relative difference between $P' = P[1000 \times 1000 \times 1000]$ and $P = P[L \times L \times L]$ for $L = 10$ (dotted red) and $L = 30$ (dashed green) as a function of the vacancy density v , and (b) a comparison between the sum $-\sqrt{v} \sum_{l=1}^L \ln \beta(l^2) = -(\sqrt{v}/3) \ln P[L \times L \times L]$ and the integral in Eq. (24), $\lambda_{3,2} + \sqrt{v}[(\ln v)/4 - 1]$, as a function of the vacancy density v for different sizes. The black continuous line is $\lambda_{3,2} + \sqrt{v}[(\ln v)/4 - 1]$. The symbols mark the critical density for $L = 10$ (red circle, $v_c \approx 0.029$), $L = 30$ (green square, $v_c \approx 0.012$), and $L = 100$ (blue triangle, $v_c \approx 0.007$). The relative difference is very small at the critical vacancy density ($v_c \approx 0.029$ for $L = 10$ at which the relative difference is 0.0003 and $v_c \approx 0.012$ for $L = 30$ at which the relative difference is 3×10^{-10}). For a given L , λ_{eff} is very close to $\lambda_{3,2} + \sqrt{v}[(\ln v)/4 - 1]$ until a certain value of the density where it drops rapidly. It is clear that for each L , around v_c the approximation is valid.

Therefore, when $l \leq L_1$, P satisfies the same equation as in a cube, Eq. (14), and the function β is given by Eq. (19). When $L_1 < l \leq L_2$ and $L_2 \leq l \leq L_3$, the probability P satisfies similar recursion relations, such that in all three cases

$$\beta(x) = \frac{1 - \rho^x + \sqrt{1 + 2\rho^x - 3\rho^{2x}}}{2}. \quad (27)$$

In order to find the critical density we use Eqs. (26) and (27) in Eq. (25),

$$\begin{aligned} 0 &= \ln V + 3 \sum_{l=1}^{L_1} \ln \beta(l^2) + 2 \sum_{l=L_1+1}^{L_2} \ln \beta(L_1 l) \\ &\quad + \sum_{l=L_2+1}^{L_3} \ln \beta(L_1 L_2), \end{aligned} \quad (28)$$

where $V = L_1 L_2 L_3$ is the volume of the system. We now change the first two sums to integrals over $z = \sqrt{v}l$ and $z = vL_1 l$, respectively, and calculate the third sum explicitly,

$$0 = \ln V - \frac{3}{\sqrt{v}} \int_{\sqrt{v}}^{\sqrt{v}L_1} g_1(z^2) dz - \frac{2}{vL_1} \int_{vL_1(L_1+1)}^{vL_1 L_2} g_1(z) dz + (L_3 - L_2) \ln \beta(L_1 L_2). \quad (29)$$

We assume that v is sufficiently small such that the lower limit of the first integral can be taken to zero. If L_3 is not too large compared to L_1 and L_2 , we can neglect the third term. Assuming again that L_1 and L_2 are large enough this last condition can be written as

$$L_3 \ll \ln^{-1} \beta(L_1 L_2) \approx \exp[2vL_1 L_2]. \quad (30)$$

For now, we assume that it is satisfied, and thus implicitly assume that $L_2 \approx L_3$, i.e., that the system has at least $d_{\text{eff}} \geq 2 = m$ and so is weakly confined. The case when this condition is not satisfied, and thus the system is strongly confined, is dealt with in the next section.

We now look at vL_1^2 and $vL_1 L_2$. If L_1 is large enough that $vL_1^2 \gg 1$, the system behaves as a cubic system, since L_1 is large enough to be considered similar to L_2 . If vL_1^2 is small but $vL_1 L_2$ is large, then the system behaves as a quasiplanar system. The third option, that $vL_1 L_2 \ll 1$, cannot exist near the critical density under the assumption that $L_2 \approx L_3$.

If $\sqrt{v}L_1 \gg 1$, the upper limit of the first integral can be taken to be ∞ and the second integral can be neglected. Thus, the equation for the critical density is

$$0 = \ln V - \frac{3\lambda_{3,2}}{\sqrt{v}}, \quad (31)$$

and the solution is

$$v_c^{\text{bulk}} = \left(\frac{3\lambda_{3,2}}{\ln V} \right)^2. \quad (32)$$

Note that in a cube $V = L^3$, and so we retrieve Eq. (1) for $m = 2$ in three-dimensional systems. This result means that in the bulk regime, the ratio between the different length scales is unimportant, and the only relevant quantity is the system's volume.

If $\sqrt{v}L_1 \ll 1$, the first integral can be neglected and the limits of the second integral can be taken to be 0 and ∞

$$0 = \ln V - \frac{2\lambda_{2,2}}{vL_1}, \quad (33)$$

such that the critical density is

$$v_c^{QP} = \frac{2\lambda_{2,2}}{L_1 \ln V}, \quad (34)$$

which is similar to the behavior of a bulk two-dimensional system,

$$v_c^{2D} = \frac{2\lambda_{2,2}}{\ln V}. \quad (35)$$

We will now consider what happens when L_3 is very large, such that $L_3 \gg \exp[2vL_1 L_2]$.

3. Strong confinement

When $L_3 \gg \exp[2vL_1 L_2]$, we cannot use the notion of critical droplets as is, but must first note that the tunnel is divided into independent sections, similarly to two-dimensional systems [62]. We note that if two or more adjacent planes lying in the short directions are completely occupied, then they are permanently frozen. We call w ($w \geq 2$) adjacent full planes a *wall* of width w . Between each two walls there are a number of planes, which do not contain two or more adjacent occupied planes, and we call these planes a *section* of length l . Each section is independent of the others, i.e., its state (whether it is frozen or not) is independent of the configuration of the other sections. We assume that each section behaves as a bulk system of size $L_1 \times L_2 \times l$, and take the average value of l as a representative for the whole system. Using combinatorial calculations very similar to those detailed in [62], we find that the relative probability of finding a section of length l is

$$Q(l) = \frac{1 - \rho^{L_1 L_2}}{\sqrt{1 + 2\rho^{L_1 L_2} - 3\rho^{2L_1 L_2}}} [\beta_+^l - \beta_-^l], \quad (36)$$

with

$$\beta_{\pm} = \frac{1 - \rho^{L_1 L_2} \pm \sqrt{1 + 2\rho^{L_1 L_2} - 3\rho^{2L_1 L_2}}}{2}. \quad (37)$$

The average section length in the L_3 direction is

$$\langle l_3 \rangle = \frac{\sum_{l=1}^{\infty} l Q(l)}{\sum_{l=1}^{\infty} Q(l)} = \rho^{-2L_1 L_2} + \rho^{-L_1 L_2} - 1 \approx \rho^{-2L_1 L_2} \approx \exp[2vL_1 L_2]. \quad (38)$$

Hence, the division into sections is valid if $L_3 > \langle l_3 \rangle$.

We can now consider a system of size $L_1 \times L_2 \times \langle l_3 \rangle$, which behaves as either a bulk system or a quasiplanar system. If it behaves as a bulk system, i.e., $\sqrt{v}L_1 \gg 1$, the critical density satisfies the equation

$$v_c^{\text{tunnel}} = \left(\frac{3\lambda_{3,2}}{\ln(L_1 L_2 \langle l_3 \rangle)} \right)^2, \quad (39)$$

which is equivalent to the following cubic equation on $\sqrt{v_c}$:

$$\ln(L_1 L_2) \sqrt{v_c} + 2L_1 L_2 v_c^{3/2} - 3\lambda_{3,2} = 0. \quad (40)$$

In the limit $L_1 L_2 \gg [\ln(L_1 L_2)]^3$, the solution to this equation is

$$v_c^{\text{tunnel}} = \left(\frac{3\lambda_{3,2}}{2L_1 L_2} \right)^{2/3}. \quad (41)$$

If the section behaves as a quasiplane, i.e., $\sqrt{v}L_1 \ll 1$, the system is a quasitunnel (QT), the critical density satisfies the equation

$$v_c^{QT} = \frac{2\lambda_{2,2}}{L_1 \ln(L_1 L_2 \langle l_3 \rangle)}, \quad (42)$$

and the solution is

$$v_c^{QT} = \frac{\sqrt{16L_1^2 L_2 \lambda_{2,2} + L_1^2 \ln^2(L_1 L_2) - L_1 \ln(L_1 L_2)}}{4L_1^2 L_2} \approx \sqrt{\frac{\lambda_{2,2}}{L_1^2 L_2}}. \quad (43)$$

If $\langle l_3 \rangle > L_2$ then there are no more divisions, since the section is built such that it is not divided further. However, if $\langle l_3 \rangle < L_2$, then *a priori* it may be that L_2 is so large that the section is again divided into subsections in the L_2 direction similarly to what was done before. In Appendix A we show that in fact the section is not divided into smaller subsections.

B. Critical density in the $m = 3$ model

We now turn to the $m = 3$ model, which is always jammed for $d = 2$ but not for $d \geq 3$. We first rederive the critical density for 3D cubes of size $L \times L \times L$ [60], again using the notion of critical droplets.

Consider an unblocked cube of size $L \times L \times L$. The cube can be expanded if the layers adjacent to its sides satisfy some condition which allows them to be unblocked. To construct these conditions, consider a system composed of two 2D layers, each layer of size $L \times L$. These layers correspond to the layers adjacent to one side of the cube. A particle on the bottom layer (the one closer to the original cube) can become unblocked if it has at least two neighboring vacancies in the two layers, and a particle on the top layer can become unblocked if it has at least three neighboring vacancies. This is similar to the 2D case with $m = 2$, so we again use the notion of a critical droplet inside the two layers. An empty rhombus of size $l \times l \times 2$ can be expanded in one direction if one of two conditions is satisfied, similarly to the $m = 2$ case: (1) At least one site in the two rows (the one on the top and the one on the bottom) adjacent to the square is empty, or (2) at least one site in the next-to-nearest bottom row is empty. Figure 5 illustrates these conditions.

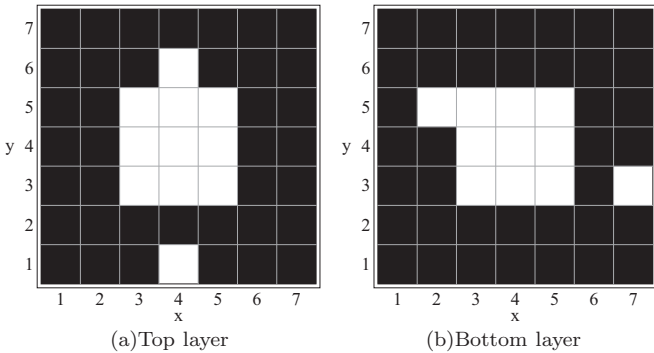


FIG. 5. An example for the two layers above the empty cube. Black squares are occupied and white squares are empty. The $3 \times 3 \times 2$ rhombus depicted here can be expanded in three of the four possible directions. The rhombus can be expanded in the positive y direction, because its top layer has an adjacent vacancy in that direction in site (4,6). It can be expanded in the positive x direction, because its bottom layer has a vacancy in the next-to-nearest column in site (7,3). It can be expanded in the negative x direction, because its bottom layer has a vacancy adjacent to it in site (2,5). It cannot be expanded in the negative y direction, because its top layer does not have an adjacent vacancy, it only has a vacancy in the next-nearest row at site (4,1), which is not enough.

Therefore, assuming that the probability of a rhombus of size $L \times L \times 2$ to be empty is

$$P_2(L \times L) = \prod_{l=1}^L \beta_3^2(l), \tag{44}$$

we find that the function $\beta_3(l)$ satisfies the recursion relation

$$\beta_3^2(l) = (1 - \rho^{2l})\beta_3(l) + \rho^{2l}(1 - \rho^l), \tag{45}$$

and is thus equal to

$$\beta_3(l) = \frac{1 - \rho^{2l} + \sqrt{(1 + \rho^{2l})^2 - 4\rho^{3l}}}{2}. \tag{46}$$

The face of the cube can be expanded if at least one of the sites on the two layers adjacent to it is a critical droplet. The entire cube can be expanded if it can be expanded in all three directions. Hence, the probability that a cube can be expanded to size $L \times L \times L$ is

$$P_3(L \times L \times L) = \prod_{l=1}^L \left[1 - \left(1 - \prod_{k=1}^l \beta_3^2(k) \right)^{2l^2} \right]^3 = \exp \left(3 \sum_{l=1}^L \ln \left\{ 1 - \left[1 - \exp \left(2 \sum_{k=1}^l \ln \beta_3(k) \right) \right]^{2l^2} \right\} \right). \tag{47}$$

Changing the sums to integrals and taking the upper limit to ∞ yields

$$P_3(L \times L \times L) \approx \exp \left[-3\mu \exp \left(\frac{\lambda_{3,3}}{v} \right) \right], \tag{48}$$

where

$$\mu = - \int_0^\infty \ln[1 - \exp(-2z^2)] dz \approx 1.6. \tag{49}$$

See Appendix B for the full details.

The critical density is found from the equation

$$1 = L^3 P_3(L \times L \times L) \Rightarrow v_c \approx \frac{\lambda_{3,3}}{\ln \ln L}. \tag{50}$$

Strong confinement in 3D rhomboids

In order to estimate the critical density in quasiplanes we consider the typical size of the unfrozen clusters. We consider only square clusters and assume that averaging over all possible shapes is the same as averaging over squares. Similarly to the $m = 2$ case in 2D, we assume that the relative probability of clusters of size l^2 is the probability of expanding a critical droplet to size $L_1 \times l \times l$. We now fix L_1 and take L_2 and L_3 to infinity, and expand a droplet. Up to size $L_1 \times L_1 \times L_1$, the expansion is the same as in a bulk system. After that, the droplet can be expanded in only two directions, and each side of the rhomboid is of size $L_1 \times l$. The probability that each side is unblocked is $\beta_3^l(L_1)$, where β_3 was defined in Eq. (46). However, the side of the rhomboid may be divided into subsections, similarly to the division of subsections in the $m = 2$ model in two dimensions, by walls consisting of two or more adjacent full walls of size $L_1 \times 2$. The average

length of these subsections is $\approx \rho^{-4L_1}$, and above that length some of the sites in the rhomboid's side are very likely to be frozen. Therefore, the characteristic size of the sections is $L_1 \times \rho^{-4L_1} \times \rho^{-4L_1}$. Note that this characteristic size does not depend on $\lambda_{3,3}$. The critical density is found from the equation

$$v_c^{QP} \approx \frac{\lambda_{3,3}}{\ln \ln L_1 \rho_c^{-8L_1}} \approx \frac{\lambda_{3,3}}{\ln(\ln L_1 + 8L_1 v_c)}. \quad (51)$$

In the limit of $8L_1 v_c \gg \ln L_1$, the solution is

$$v_c^{QP} = \frac{1}{W_0(8\lambda_{3,3}L_1)} \approx \frac{1}{\ln(8\lambda_{3,3}L_1)}, \quad (52)$$

where $W_0(x)$ is the product-log function [65].

When the system is confined to a tunnel, the side of the rhomboid is not divided into subsections, because it is of constant size $L_1 \times L_2$. In that case, the tunnel is divided into sections by walls, which are one or more adjacent planes of size $L_1 \times L_2$ that are frozen. Assuming that L_1 and L_2 are large enough, the probability that a plane is frozen is $1 - \exp[-L_1 L_2 \exp(-2\lambda_{3,3}/v)]$. This is very similar to a tunnel in the $m = 2$ model in which the probability that a plane is frozen is $1 - \rho^{L_1 L_2} \approx 1 - \exp(-v L_1 L_2)$. Therefore, we can use the known results for tunnels in $m = 2$ and replace v with $\exp(-\lambda_{3,3}/v)$. The average section length is

$$\langle l \rangle \approx \exp[L_1 L_2 \exp(-2\lambda_{3,3}/v)]. \quad (53)$$

The critical density is found from the equation

$$v_c^{\text{tunnel}} \approx \frac{\lambda_{3,3}}{\ln \ln (L_1 L_2 \langle l \rangle)}, \quad (54)$$

and thus

$$v_c^{\text{tunnel}} \approx \frac{3\lambda_{3,3}}{\ln(L_1 L_2)}. \quad (55)$$

III. JAMMING BY SHAPE IN 3D RHOMBOIDS IN THE $m = 2$ MODEL

In this section we show how changing only the shape of the system can change its behavior and induce jamming. Although we show this only for three-dimensional systems in the $m = 2$ model, the conclusions are valid for any dimension and any m .

We focus on four possible relations between the three length scales L_1, L_2 , and L_3 . If $L_1 \approx L_2 \approx L_3$ the system behaves as a cubic (bulk) system. If $L_1 \ll L_2 \approx L_3$ we call the system a quasiplanar (QP) system. If $L_1 \approx L_2 \ll L_3$ the system is a tunnel. If $L_1 \ll L_2 \ll L_3$ we call the system a quasitunnel (QT). The critical vacancy densities in the four regimes are given by (see Sec. II A)

$$v_c^{\text{bulk}} = \left(\frac{3\lambda_{3,2}}{\ln V} \right)^2, \quad v_c^{QP} = \frac{2\lambda_{2,2}}{L_1 \ln V}, \quad (56)$$

$$v_c^{\text{tunnel}} = \left(\frac{3\lambda_{3,2}}{2L_1 L_2} \right)^{2/3}, \quad v_c^{QT} = \sqrt{\frac{\lambda_{2,2}}{L_1^2 L_2}}.$$

Bulk ($d_{\text{eff}} = 3$) and QP ($d_{\text{eff}} = 2$) systems are weakly confined, while tunnels ($d_{\text{eff}} = 1, t = 0$) and QT ($d_{\text{eff}} = 1, t = 1$) systems are strongly confined. As noted before, a strongly confined system is divided into clusters. In the $m = 2$ model, we call these clusters *sections*, as they behave

somewhat differently than do clusters in the $m > 2$ models. Only in the $m = 2$ model are the sections independent of each other, in the manner that the state of a section (whether it is frozen or not) is completely independent of the state of the neighboring sections. These sections are separated by at least two adjacent fully occupied planes perpendicular to the long direction.

By changing the different length scales L_1, L_2, L_3 for fixed volume $V = L_1 L_2 L_3$, the system crosses over between the different regimes. For example, by changing the value of L_1 , the system will cross over from bulk behavior to quasiplanar behavior. This transition occurs when the critical density satisfies both the bulk equation and the QP equation. Equating the two yields the crossover length for L_1 :

$$L_1^{\text{bulk-QP}} = \frac{2\lambda_{2,2}}{9\lambda_{3,2}^2} \ln V. \quad (57)$$

Similarly, by decreasing L_3 , the system will change from a tunnel into a bulk system or from a quasitunnel into a quasiplane. By equating the relevant expressions for the critical density we find that the crossover length is

$$L_3^{\text{bulk-tunnel}} = \frac{\exp[(18\lambda_{3,2}^2 L_1 L_2)^{1/3}]}{L_1 L_2}. \quad (58)$$

In Sec. II A, we showed that the average section size is equal to $L_3^{\text{bulk-tunnel}}$. Hence, the transition between bulk and tunnel occurs at the point where the system contains on average one section. The third crossover length is between tunnels and quasitunnels,

$$L_1^{\text{QT-tunnel}} = \left(\frac{2\lambda_{2,2}^{3/2}}{3\lambda_{3,2}} \right)^2 \sqrt{L_2}. \quad (59)$$

To show this behavior graphically, we define the three following parameters describing the shape of the system:

$$q_1 = \left(\frac{9\lambda_{3,2}^2}{2\lambda_{2,2}} \right)^3 \frac{L_1^3}{\ln^3 V},$$

$$q_2 = \left(\frac{9\lambda_{3,2}^2}{4\lambda_{2,2}^3} \right)^2 \frac{L_1^2}{L_2}, \quad (60)$$

$$q_3 = 18\lambda_{3,2}^2 \frac{L_1 L_2}{\ln^3 V},$$

such that $q_1 > 1$ implies $L_1 > L_1^{\text{bulk-QP}}$, $q_2 > 1$ implies $L_1 > L_1^{\text{QT-tunnel}}$, and $q_3 > 1$ implies $L_3 < L_3^{\text{bulk-tunnel}}$. Also, we note that $q_2 q_3 = q_1 / \lambda_{2,2}^3$. Therefore, the state of the system can be determined by any two of the three parameters q_1, q_2 , and q_3 , as shown in Fig. 6.

As each regime has a different critical density, by changing the system's shape but not its volume or density, a system may become jammed if the density was lower than the critical density at the original shape, but higher than the critical density at the new shape. Consider a system of size $W \times L \times L$ and define the aspect ratio $r = L/W$. The system has constant volume $V = WL^2$ and constant density, ρ . By changing the aspect ratio between 0 and ∞ the system changes from a tunnel ($r \ll 1$) to a bulk system ($r \approx 1$) and to a quasiplane ($r \gg 1$).

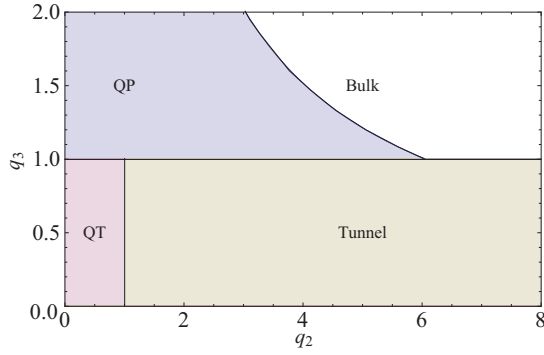


FIG. 6. (Color online) Phase diagram of the four possible states of a 3D system (bulk, QP, tunnel, and QT), as a function of the two shape parameters $q_2 = (9\lambda_{3,2}^2/4\lambda_{2,2}^3)^2(L_1^2/L_2)$ and $q_3 = 18\lambda_{3,2}^2L_1L_2/\ln^3 V$.

These transitions can be seen in Fig. 7, where the aspect ratio is changed in a system of volume $V = 10^6$ and density $\rho = 0.99$. This density was chosen so that the bulk system is unjammed, but the tunnel and quasiplanar systems are jammed. In the KA model in the bulk, the chosen density is very close to the critical density $\rho \approx \rho_c$ and so $n_F \approx 0.2$ and not 0 or 1. Even near ρ_c , n_F does not change much with r and depends only on V as long as the system is in the bulk regime. Fluctuations in n_F appear since V is not exactly the same for all aspect ratios, but varies from $V = 994\,194$ at $L = 171$ to $V = 1\,011\,240$ at $L = 159$, since the system must be a rhomboid.

In general, for a given volume V and density ρ there are four possible behaviors: (1) neither a tunnel, nor a 2D plane, nor a cube is jammed; (2) a tunnel is jammed, but not a plane or a cube; (3) a tunnel and a plane are jammed, but not a cube; (4) all

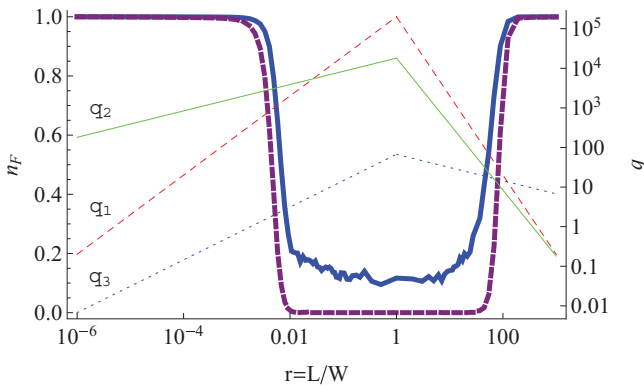


FIG. 7. (Color online) Average fraction of frozen particles n_F and the three q parameters vs aspect ratio $r = L/W$ for a system of constant volume $V = WL^2 = 10^6$ and particle density $\rho = 0.99$. The thick lines are n_F for the KA (blue solid line) and FA (purple dashed line) models, while the thin lines are the q_1 (red dashed), q_2 (green solid), and q_3 (blue dotted) parameters. The system changes from tunnel to bulk at $r \approx 0.01$ ($W \approx 2100$, $L \approx 21$, $q_3 = 1$) and from bulk to quasiplanar at $r \approx 70$ ($W \approx 6$, $L \approx 420$, $q_1 \approx 10$). The value of q_1 at the transition from bulk to quasiplanar is not 1 but larger, because the values of the λ parameters are far from their asymptotic values.

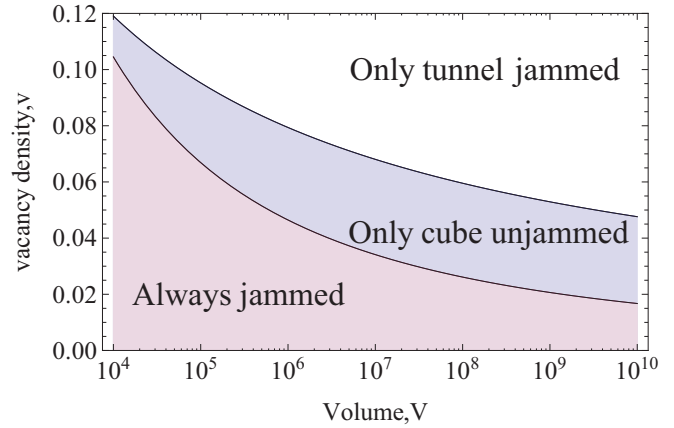


FIG. 8. (Color online) The behavior of a 3D system in the $m = 2$ models as a function of its volume and vacancy density. This plot was drawn using the asymptotic values of $\lambda_{2,2}$ and $\lambda_{3,2}$. If we knew their values for any volume and density, the plot would be more accurate. Hence, the values chosen in Fig. 7 ($V = 10^6$, $v = 0.01$) appear here in the “Always jammed” region, while they should be in the “Only cube unjammed” region.

possible shapes are jammed. The first behavior, that a tunnel is unjammed, occurs only for very low densities, since the critical density of an infinite tunnel is approximately 0.3 [62], and the critical densities for large planes and cubes are much higher. Therefore, we disregard that possibility. By varying either the system’s volume or the particle density, the behavior of the system changes among the other three possibilities. The crossover occurs along the lines in which the density is equal to the critical density for 2D planes of that volume and for cubes of that volume. Note that for each combination of volume and density, the transition between bulk and quasiplanes occurs at a different aspect ratio. Figure 8 shows the behavior of the system as a function of its volume and vacancy density.

The crossover from QP behavior to bulk behavior is illustrated in Fig. 9(a), which shows $\sqrt{v_c} \ln V$ as a function of W for systems of size $W \times 10^3 \times 10^3$. When $W \geq 15$, the value of $\sqrt{v_c} \ln V$ is approximately constant, which fits the behavior of bulk systems; see Eq. (56). In QP systems, we see from Eq. (56) that $\sqrt{v_c} \ln V \sim \sqrt{\ln(V)/W}$ which qualitatively agrees with the results for $W \leq 15$. However, for small values of W the simulation results do not scale as expected, because in these relatively small systems the effective value of λ depends strongly on the system’s size.

Figure 9(b) shows the critical vacancy density of tunnels of size $W \times W \times L$, where L is large enough so that the system is practically infinitely long. We see that the results from the simulations agree with the exact solution of Eq. (40). In order to see the scaling of $v_c^{\text{tunnel}} \sim W^{-4/3}$, the condition $W^2 \gg 8(\ln W)^3$ should be satisfied. Our results are only up to $W = 29$, for which $W^2 = 841$ and $8(\ln W)^3 \approx 300$, and so the asymptotic scaling is not satisfactory. In order to get, say, $W^2 = 10 \times 8(\ln W)^3$, we need to go to $W = 83$, which requires a system of length $L \approx 10^9$ to be considered infinite, and thus approximately 1 Pbyte (10^6 Gbytes) of memory.

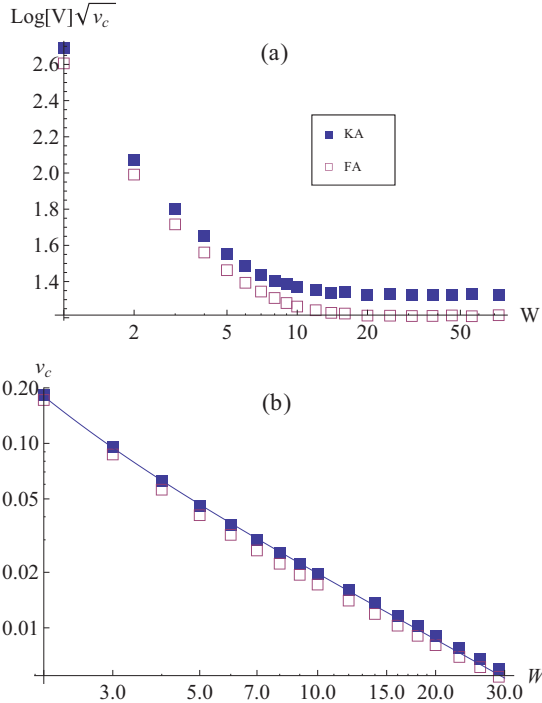


FIG. 9. (Color online) (a) The value of $3\lambda_{3,2} = \sqrt{v_c} \ln V$ as a function of W for systems of size $W \times 10^3 \times 10^3$ for the KA and FA models. Above $W \geq 15$, $\lambda_{3,2}$ does not depend on W , which fits the behavior of a bulk system. Below $W \leq 15$, the system is a quasiplane so it does not correspond to the bulk behavior. (b) The critical vacancy density v_c for tunnels of size $W \times W \times L$ as a function of the width W for the KA and FA models. The length L is long enough for the tunnel to be considered infinite ($L = 10^3$ for $W \leq 9$, $L = 2 \times 10^3$ for $W \leq 16$, $L = 4 \times 10^3$ for $W = 18$, $L = 2 \times 10^4$ for $W = 20, 23$, $L = 5 \times 10^4$ for $W = 26$, and $L = 2 \times 10^5$ for $W = 29$). The continuous line is the value of v_c according to Eq. (40) with $\lambda_{3,2} = 0.4$.

IV. STRONGLY CONFINED 3D RHOMBOIDS IN THE $m = 3$ MODEL

A. The correlation length

In the $m = 3$ model, a strongly confined system is divided into frozen clusters which are not independent. Consider a “view from above” on a three-dimensional system, such that it appears to be a two-dimensional system, say in the x - y plane. Each “site” in this effectively 2D system represents a column which is either completely full or not. Any closed shape formed by full columns is frozen, and the sites confined by this wall are independent of the sites outside the wall. The most probable closed shape is a 2×2 square. If two such vertical pillars are close to each other, there is a possibility that they are connected by a horizontal scaffold, which is also frozen if it is at least two sites wide. These scaffolds can also connect between themselves, and thus form frozen clusters. The clusters are not completely independent, but their correlation decreases with the distance between them. Figure 10 shows an example of a configuration and the frozen sections in it. The 2D projection of the frozen clusters is very similar to the results of continuous models in 2D [66], in which particles form dense regions reminiscent of our frozen clusters.

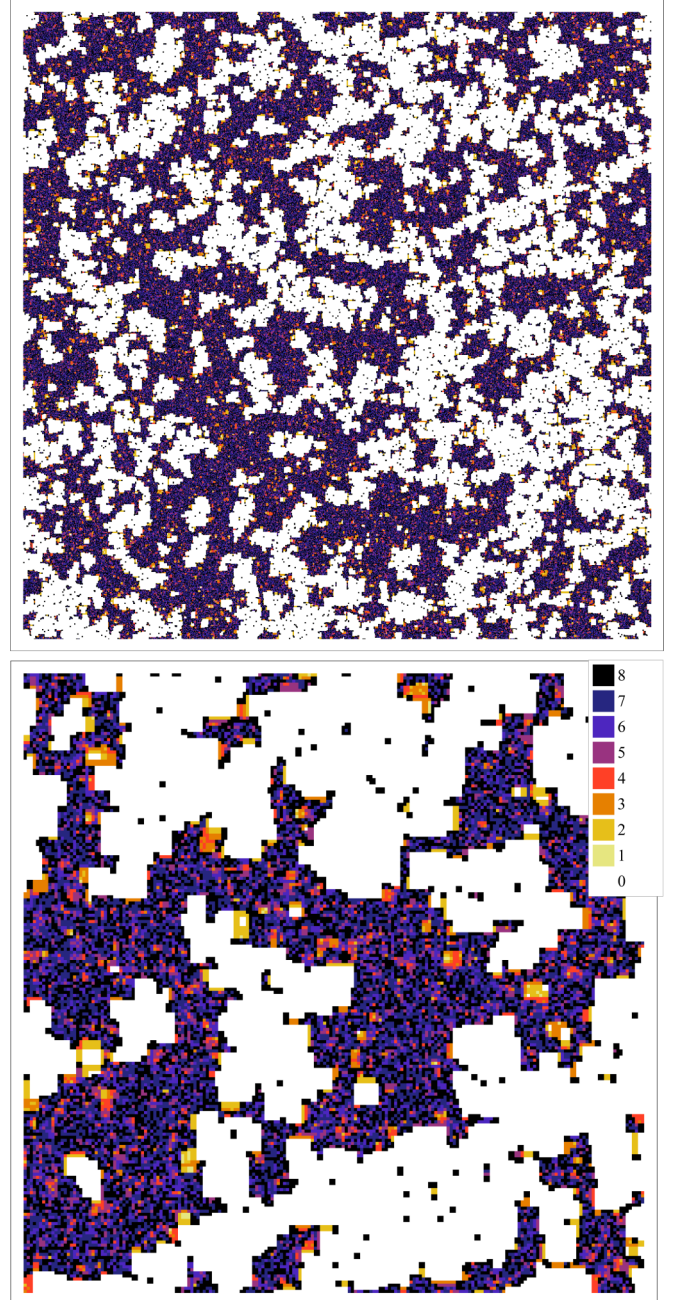


FIG. 10. (Color online) Two-dimensional projection of the frozen particles in a system of size $1000 \times 1000 \times 8$ in the FA model with $m = 3$ with periodic boundary conditions. The density is $\rho = 0.881$ and the fraction of frozen particles is $n_F = 0.46$. The colors represent the number of frozen particles in each column, as shown in the lower panel. The full columns do not create closed sections, but when they are close they create a frozen cluster by scaffolding. The second panel is a zoom-in on a portion 200×200 of the projection.

Moreover, with hard-wall boundary conditions both the frozen clusters in the KA and FA models and the dense regions in the continuous model form near the edges of the system.

As an approximation, we consider the frozen areas as adjacent frozen clusters of typical size ξ , and similarly for

the unfrozen areas. We assume that at the critical density, the typical size of the frozen and unfrozen clusters is the same. We further assume that the typical cluster size is equal to the correlation length between frozen sites. In order to obtain the correlation length, we assume that the correlation between sites \vec{i} and \vec{j} being frozen decreases exponentially with their distance:

$$c_{\vec{i},\vec{j}} = \rho n_F (1 - \rho n_F) \exp\left[-\frac{|\vec{i} - \vec{j}|}{\xi}\right]. \quad (61)$$

The numerical results, shown in Fig. 11(a), support this assumption. Finding the correlation length numerically using Eq. (61) is very costly. Instead, we find it using a related quantity which is easier to evaluate numerically, namely, the average correlation in the system,

$$C_{av} = \frac{1}{V^2} \sum_{\vec{i},\vec{j}} c_{\vec{i},\vec{j}} = \frac{c_0}{V} \sum_{x,y,z} \exp[-\sqrt{x^2 + y^2 + z^2}/\xi], \quad (62)$$

where $c_0 = \rho n_F (1 - \rho n_F)$, x, y, z are the distances along the three directions between two sites, and when using periodic boundary conditions, the three sums are from $-[(L_i + 1)/2] + 1$ to $[L_i/2]$, with $[q]$ being the integer part of q .

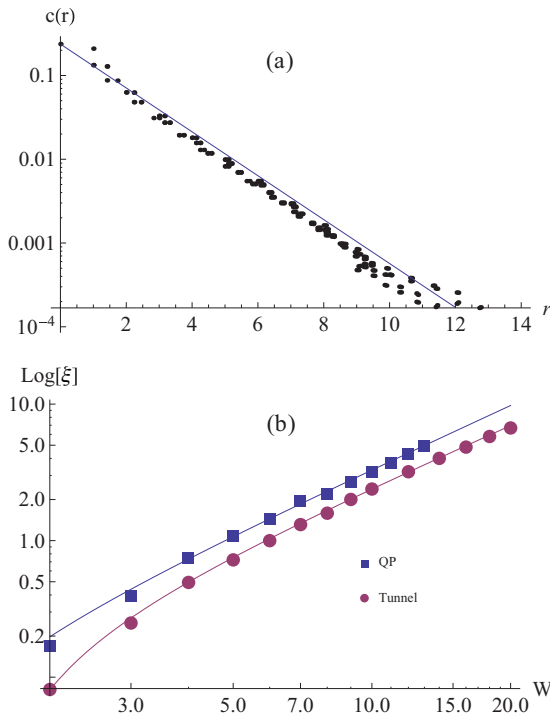


FIG. 11. (Color online) (a) The correlation $c_{\vec{i},\vec{j}}$ as a function of the distance $r = |\vec{i} - \vec{j}|$ for a quasiplane of size $3 \times 100 \times 100$ in the FA model near the critical density $\rho = 0.81$. The straight line is $\rho n_F (1 - \rho n_F) \exp[-r/\xi]$, with $\xi \approx 1.66$ calculated by the fluctuations in n_F . The deviation from the line is due to the large weight of the few nearby points whose correlation requires corrections to the exponential decay. (b) The estimated correlation length ξ as a function of the width W for quasiplanes of size $W \times \infty \times \infty$ (blue squares) and tunnels of size $W \times W \times \infty$ (red circles) at the critical density. The continuous lines are a fit to $\xi = \gamma_1 \exp[\gamma_2 W^{\gamma_3}]$.

Appendix D shows that C_{av} is related to the fluctuations in the fraction of frozen particles n_F between different configurations by

$$C_{av} = \sigma^2 = \frac{1}{A} \sum_{\alpha} (\rho n_F^{\alpha})^2 - \left(\frac{1}{A} \sum_{\alpha} \rho n_F^{\alpha} \right)^2, \quad (63)$$

where the summation is over A different realizations α of the system, and n_F^{α} is the fraction of frozen particles in configuration α .

In quasiplanes, we assume that $L_2, L_3 \gg \xi$, such that the sums of y and z in Eq. (62) may be changed to integrals with the limits of the integrals taken to infinity. We now change the integration variables from y and z to $r = \sqrt{y^2 + z^2}$ and $\theta = \tan^{-1} z/y$, such that

$$\begin{aligned} C_{av}^{QP} &= \frac{c_0}{V} \sum_x \int_0^{\infty} \int_0^{2\pi} r dr d\theta \exp[-\sqrt{x^2 + r^2}/\xi] \\ &= \frac{2\pi c_0}{V} \sum_{x=-[(L_1+1)/2]+1}^{[L_1/2]} \xi(\xi + |x|) \exp[-|x|/\xi] \\ &= \frac{\pi \xi c_0}{V \sinh^2(1/2\xi)} \left\{ 1 + \xi \sinh(1/\xi) \right. \\ &\quad \left. - \exp\left[-\frac{[L_1/2]}{\xi}\right] [1 + (\xi + [L_1/2]) \right. \right. \\ &\quad \left. \left. \times (\sinh(1/\xi) - 2\delta_{L_1, \text{odd}} \sinh^2(1/2\xi)) \right] \right\}. \quad (64) \end{aligned}$$

For wide quasiplanes we find that $\xi \gg L_1$, such that

$$C_{av}^{QP} \approx \frac{2\pi \xi^2 L_1 c_0}{V}. \quad (65)$$

In tunnels we assume that $L_3 \gg \xi$, such that the sum of z in Eq. (62) may be changed to an integral with the limits of the integral taken to infinity. Hence

$$\begin{aligned} C_{av}^{tun} &= \frac{c_0}{V} \sum_{x,y} \int_{-\infty}^{\infty} \exp[-\sqrt{x^2 + y^2 + z^2}/\xi] dz \\ &= \frac{2c_0}{V} \sum_{x,y} \int_0^{\infty} \exp[-\sqrt{x^2 + y^2 + z^2}/\xi] dz. \quad (66) \end{aligned}$$

Changing the integration variable to $r = \sqrt{x^2 + y^2 + z^2}$ yields

$$\begin{aligned} C_{av}^{tun} &= \frac{2c_0}{V} \sum_{x,y} \int_{\sqrt{x^2+y^2}}^{\infty} \exp[-r/\xi] \frac{r dr}{\sqrt{r^2 - x^2 - y^2}} \\ &= \frac{2c_0}{V} \sum_{x,y} \sqrt{x^2 + y^2} K_1\left(\frac{\sqrt{x^2 + y^2}}{\xi}\right), \quad (67) \end{aligned}$$

where K_1 is the modified Bessel function of the second kind [67]. The sums over x and y are done numerically. In wide tunnels, we also find that $\xi \gg L_1, L_2$, such that $r K_1(r/\xi) \approx \xi$, and thus

$$C_{av}^{tun} \approx \frac{2c_0 \xi}{V} \sum_{x,y} 1 = \frac{2\xi L_1 L_2 c_0}{V}. \quad (68)$$

TABLE I. The values of the γ parameters obtained by the numerical fit to $\xi = \gamma_1 \exp[\gamma_2 W^{\gamma_3}]$ at the critical density.

	γ_1	γ_2	γ_3
Quasiplane	0.923	0.0948	1.55
Tunnel	0.861	0.0861	1.49

By calculating σ^2 numerically, and using Eq. (63) and either Eq. (64) (for quasiplanes) or (67) (for tunnels), we found the correlation length ξ . We fitted the value of ξ to a function of the form

$$\xi = \gamma_1 \exp[\gamma_2 W^{\gamma_3}], \quad (69)$$

where W is the width of the system for either a quasiplane of size $W \times \infty \times \infty$ or a tunnel of size $W \times W \times \infty$. The result is shown in Fig. 11(b). As shown in Table I, the values of the γ parameters for quasiplanes and tunnels are similar. Note that the correlation length in Eq. (69) has a similar functional form as the average section length in tunnels in the $m = 2$ model (see Sec. II A)

$$\langle l \rangle = \exp[2^{-1/d} (d\lambda_{d,2})^{1-1/d} W^{1-1/d}], \quad (70)$$

such that for $d = 3$, $\gamma_1 = 1$, $\gamma_2 \approx 1.64$, and $\gamma_3 = 2/3$.

As an approximation, we assume that a cluster of size ξ is unfrozen if it contains a critical droplet, such that the critical density may be obtained for large W from the relation

$$1 = \xi^2 W P[\xi \times \xi \times W] \quad (71)$$

for quasiplanes, and

$$1 = \xi W^2 P[\xi \times W \times W] \quad (72)$$

for tunnels. Solving these equations for large W yields in both cases

$$v_c = \frac{\lambda_{3,3}}{\gamma_3 \ln W}, \quad (73)$$

which is of the same functional form as the critical density for two-dimensional systems in the $m = 2$ model but with a different prefactor, and agrees qualitatively with Eqs. (52) and (55). Interestingly, we obtain the same expression for quasiplanes and for tunnels. We cannot compare Eq. (73), which is valid for very large systems, to our numerical results, because our simulations are done on relatively small systems ($W = 13$ for QPs and $W = 20$ for tunnels) in which the effective value of $\lambda_{3,3}$ varies significantly and is very far from its asymptotic value.

B. Transition from bulk to quasiplanar behavior

Since the critical density changes very slightly in the system sizes we investigated, another technique was used to see the crossover between bulk and quasiplanar behavior. In the bulk, the system is either almost completely unfrozen or almost completely frozen, and thus its probability of being frozen can be approximated by a binary distribution. In this case, the variance σ^2 of the fraction of frozen particles over many configurations is approximately $\sigma^2 \approx n_F(1 - n_F)$, or $1/4$ at the critical density. In a two-dimensional system, however, the frozen structures are very local, and thus a large enough system can in itself be considered an average

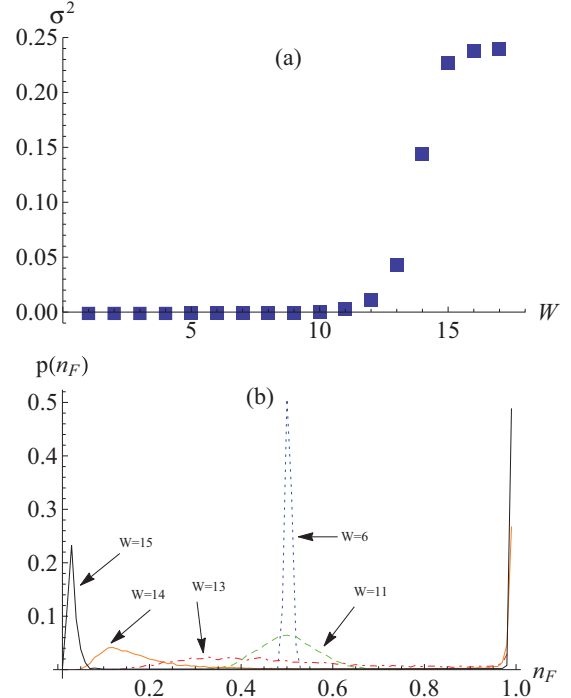


FIG. 12. (Color online) (a) The variance σ^2 in the fraction of frozen particles and (b) the distribution $p(n_F)$ at the critical density for a system of size $W \times 1000 \times 1000$ in the $m = 3$ FA model. For small width ($W = 6, \rho_c = 0.8536$, blue dotted curve) there is a sharp peak around 0.5. Near the crossover region ($W = 11, \rho_c = 0.88806$, green dashed curve) the peak is still visible, but is much broader. During the crossover ($W = 13, \rho_c = 0.89661$, red dash-dotted curve) the distribution almost flattens, but the emergence of the peak at 1 can be seen. At $W = 14$ ($\rho_c = 0.90006$, orange solid curve) the peak at 1 is clearly seen, and a broad peak centered around 0.1 is also visible. As the width is further increased ($W = 15, \rho_c = 0.90205$, black solid curve) the system shows almost bulk behavior and the two peaks at 1 and near 0 are obvious. At that point ($W = 15$) there is a crossover from quasiplanar behavior, in which $\sigma^2 \approx 0$, to a bulk behavior, in which $\sigma^2 \approx 1/4$.

over many small systems. In this case, the distribution of n_F over the different configurations is almost constant and thus the variance is almost zero. The distribution of n_F and its variance at the critical density are plotted in Fig. 12 for a system of size $W \times 1000 \times 1000$. At that size, the crossover occurs at $W \approx 15$, which means that for systems of width 15, the characteristic size of the sections is of the same order of magnitude as the system size. The characteristic cluster size, calculated by Eq. (69) is approximately $\xi \approx 500$, which is expected given the system size ($L = 1000$). For small widths ($W \leq 11$), there is a pronounced peak in the distribution at 0.5, which becomes broader as the width increases. At larger widths, the emergence of the two peaks at 0 and 1 is visible. Note also that the distribution is not symmetric: while the peak at 1 is very large, the peak near 0 is broad and is centered around a small positive value, which nears 0 as the width increases. This means that the number of frozen particles in the almost unfrozen configurations vary, while those that are almost completely frozen have very small and negligible unfrozen regions.

V. SUMMARY

In this paper we investigated the effects of the system's shape on the jamming transition. We derived an analytical approximation for the critical density in a d -dimensional hyper-rhomboid system in both the Kob-Andersen and Fredrickson-Andersen kinetically constrained models, and showed that it scales differently with the system's length scales depending on the relation between them. We distinguished between two general classes of systems depending on the model's parameter m and the number of effective dimensions in the systems, d_{eff} : a weakly confined system ($d_{\text{eff}} \geq m$) and a strongly confined system ($d_{\text{eff}} < m$). In the weakly confined regime, the system is either completely unfrozen or almost completely frozen, and the correlation length between frozen sites is the entire system size. The critical density in a weakly confined system depends on the volume of the system V and the volume associated with the s small dimensions V_s , but not on the ratios between the small dimensions or the large dimensions. In the strongly confined regime, the system is divided into frozen and unfrozen clusters, such that the correlation length between frozen sites is the size of the clusters, not of the system. The critical density in a strongly confined system depends on V_s , but not on the large dimensions or the ratios between the small dimensions.

We also showed how changing the system's shape without altering its total volume or the particle density can induce jamming. This was done by utilizing our result that the critical density depends on the system's shape, such that a certain density may be below the critical density at a particular shape but above it for a different shape. We emphasize that this is derived by averaging over ensembles of different realizations, not by exerting forces on the system. Although we considered only the Kob-Andersen and the Fredrickson-Andersen models, this conclusion may be applicable to other models as well, including continuous models. It may be interesting to investigate this phenomenon in other, more physical, kinetically constrained models such as the Jäckle-Krönig model [27] on the triangular lattice, the east model [41], the north-east model [42], or the spiral model [32].

The results presented in this paper regarding the effect of the shape on the static properties of the models will be the groundwork for an investigation of the effect of the shape on the dynamic properties of these models.

ACKNOWLEDGMENTS

We thank Roman Golkov and Itai Einav for helpful discussions. This research was supported by the Israel Science Foundation Grants No. 617/12 and No. 1730/12.

APPENDIX A: PROOF THAT SECTIONS IN THE $m = 2$ MODELS IN $d = 3$ CANNOT BE FURTHER DIVIDED

In order for a section to be divided into subsections, it needs to satisfy the condition

$$L_2 > \exp[2vL_1 \langle l_3 \rangle], \quad (\text{A1})$$

or equivalently

$$vL_1 < \frac{W_0(L_2 \ln L_2)}{2L_2}, \quad (\text{A2})$$

where $W_0(z)$ is the product-log function [65] defined as the solution to

$$z = W_0(z) \exp[W_0(z)]. \quad (\text{A3})$$

For large L_2 we can approximate this by

$$vL_1 < \frac{\ln L_2}{2L_2}. \quad (\text{A4})$$

The critical vacancy density in this case is larger than or equal to that of a tunnel (because the subsection is smaller and thus easier to jam), and so the condition can be written as

$$\left(\frac{3\lambda_{3,2}}{2L_1L_2}\right)^{2/3} L_1 < vL_1 < \frac{\ln L_2}{2L_2}, \quad (\text{A5})$$

or equivalently

$$L_1 < \frac{\ln^3 L_2}{9\lambda_{3,2}^2 L_2}. \quad (\text{A6})$$

The right-hand side is bounded by $3/(e^3 \lambda_{3,2}^2) \approx 0.15$. This means that L_1 cannot possibly satisfy the condition, and therefore no further partitions are possible.

APPENDIX B: CALCULATION OF P_3

In this section we show that

$$P_3(L \times L \times L) \approx \exp\left[-3\mu \exp\left(\frac{\lambda_{3,3}}{v}\right)\right]. \quad (\text{B1})$$

In Eq. (47), the contribution to the main sum from small l is negligible, so we can take the upper limit of the inner sum on k to be ∞ and approximate it by an integral over $z = kv$, using the approximation $\rho^k \approx e^{-vk}$,

$$\begin{aligned} P_3(L \times L \times L) &= \exp\left(3 \sum_{l=1}^L \ln\left\{1 - \left[1 - \exp\left(-\frac{2}{v} \int_0^\infty g_2(z) dz\right)\right]^{2l^2}\right\}\right) \\ &= \exp\left(3 \sum_{l=1}^L \ln\left\{1 - \left[1 - \exp\left(-\frac{2\lambda_{3,3}}{v}\right)\right]^{2l^2}\right\}\right) \\ &\approx \exp\left(3 \sum_{l=1}^L \ln\left\{1 - \exp\left[-2l^2 \exp\left(-\frac{2\lambda_{3,3}}{v}\right)\right]\right\}\right). \end{aligned} \quad (\text{B2})$$

We now change the sum over l to an integral over $z = l \exp[-\frac{\lambda_{3,3}}{v}]$ and take the upper limit to be ∞ ,

$$\begin{aligned} P_3(L \times L \times L) &\approx \exp\left\{3 \exp\left(\frac{\lambda_{3,3}}{v}\right) \int_0^\infty \ln[1 - \exp(-2z^2)] dz\right\} \\ &= \exp\left[-3\mu \exp\left(\frac{\lambda_{3,3}}{v}\right)\right], \end{aligned} \quad (\text{B3})$$

where

$$\mu = - \int_0^\infty \ln[1 - \exp(-2z^2)] dz \approx 1.6. \quad (\text{B4})$$

APPENDIX C: DERIVATION OF THE CRITICAL DENSITY IN HYPER-RHOMBOIDS

1. Hyper-rhomboids in the $m = 2$ model

We consider a hyper-rhombus of size $L_1 \times \dots \times L_d$, such that $L_{i+1} \geq L_i$ for all i . The treatment here is very similar to that in the three-dimensional case. For brevity we define

$$V_k = \prod_{i=1}^k L_i. \quad (\text{C1})$$

The expansion of the critical droplet is done analogously to the three-dimensional case such that the probability of the hyper-rhomboid to be unfrozen is

$$P = \prod_{i=1}^d \prod_{l=L_{i-1}+1}^{L_i} \beta^{d-i+1} (l^{d-i} V_{i-1}), \quad (\text{C2})$$

where $L_0 = 0$ and $V_0 = 1$. Setting this in the recursion relation on P yields

$$\beta(x) = \frac{1 - \rho^x + \sqrt{1 + 2\rho^x - 3\rho^{2x}}}{2}. \quad (\text{C3})$$

The equation for the critical density is then

$$\begin{aligned} 0 &= \ln V_d + \sum_{i=1}^d (d-i+1) \sum_{l=L_{i-1}+1}^{L_i} \ln \beta(l^{d-i} V_{i-1}) \\ &\approx \ln V_d - \sum_{i=1}^d \frac{d-i+1}{(vV_{i-1})^{1/(d-i)}} \int_{(vV_{i-1})^{1/(d-i)} (L_{i-1}+1)}^{(vV_{i-1})^{1/(d-i)} L_i} g_1(z^{d-i}) dz. \end{aligned} \quad (\text{C4})$$

We now check whether the system is divided into sections or not. It is not divided if $L_d < \langle l_d \rangle$, for which

$$\langle l_d \rangle = \exp(2vV_{d-1}). \quad (\text{C5})$$

Assuming that it is not divided, we further assume that there is a $0 \leq s < d-1$ such that $(vV_{s-1})^{1/(d-s)} L_s \ll 1$ and

$(vV_s)^{1/(d-s-1)} L_{s+1} \gg 1$. Then we can approximate Eq. (C4) by

$$\begin{aligned} 0 &= \ln V_d - \frac{d-s}{(vV_s)^{1/(d-s-1)}} \int_0^\infty g_1(z^{d-s-1}) dz \\ &= \ln V_d - \frac{(d-s)\lambda_{d-s,2}}{(vV_s)^{1/(d-s-1)}}. \end{aligned} \quad (\text{C6})$$

The critical density in this case is

$$v_c = \frac{1}{V_s} \left(\frac{(d-s)\lambda_{d-s,2}}{\ln V_d} \right)^{d-s-1}, \quad (\text{C7})$$

which is similar to the behavior of a hypercube in $d_{\text{eff}} = d-s$ dimensions with a single length scale, Eq. (1).

If the system is divided into sections, i.e., $L_d > \langle l_d \rangle$, it is not further divided into smaller subsections for the exact same reasons as in three-dimensional systems. We can again assume that there is a $0 \leq t < d-1$ that satisfies the above conditions, such that the critical density satisfies the equation

$$v_c = \frac{1}{V_t} \left(\frac{(d-t)\lambda_{d-t,2}}{\ln(V_{d-1} \langle l_d \rangle)} \right)^{d-t-1}. \quad (\text{C8})$$

If V_{d-1} is large enough such that $\ln V_{d-1} \ll 2v_c V_{d-1}$, the solution to Eq. (C8) can be approximated by

$$v_c = \frac{1}{V_t} \left(\frac{(d-t)\lambda_{d-t,2}}{2V_{d-1}} \right)^{1-1/(d-t)}. \quad (\text{C9})$$

2. Hyper-rhomboids in the $m = 3$ model

We consider a hyper-rhomboid of arbitrary size and repeat the derivation of the critical droplet. In a hyper-rhomboid, each hyperside consists of two layers which must be unblocked. Up to size L_1 , the derivation is the same as in the bulk. Above that size and up to size L_2 , there are only $d-1$ directions to consider, and one of the sides of the hyperside is set to L_1 . Above L_2 , there are only $d-2$ sides, etc. In analogy to the derivation of critical droplets in cubes, Eq. (47), and in hyper-rhomboids in the $m = 2$ models, Eq. (C2), the probability that a site is part of a critical droplet is

$$\begin{aligned} P_3 &= \prod_{l=1}^{L_1} \left[1 - \left(1 - \prod_{k=1}^l \beta_3^{d-1} (k^{d-2}) \right)^{2l^{d-1}} \right]^d \prod_{l=L_1+1}^{L_2} \left[1 - \left(1 - \prod_{k=1}^l \beta_3^{d-2} (k^{d-3} L_1) \right)^{2l^{d-2} L_1} \right]^{d-1} \\ &\quad \times \dots \times \prod_{l=L_{d-2}+1}^{L_{d-1}} \left[1 - \left(1 - \prod_{k=1}^l \beta_3 (V_{d-2}) \right)^{2l V_{d-2}} \right]^2 \\ &= \prod_{i=1}^{d-1} \prod_{l=L_{i-1}+1}^{L_i} \left[1 - \left(1 - \prod_{k=1}^l \beta_3^{d-i} (k^{d-1-i} V_{i-1}) \right)^{2l^{d-i} V_{i-1}} \right]^{d+1-i}. \end{aligned} \quad (\text{C10})$$

The equation for the critical density is

$$\begin{aligned} 0 &= \ln V_d + \sum_{i=1}^{d-1} (d-i+1) \sum_{l=L_{i-1}+1}^{L_i} \ln \left\{ 1 - \left[1 - \exp \left((d-i) \sum_{k=1}^l \ln \beta_3 (k^{d-i-1} V_{i-1}) \right) \right]^{2l^{d-i} V_{i-1}} \right\} \\ &\approx \ln V_d + \sum_{i=1}^{d-1} (d-i+1) \sum_{l=L_{i-1}+1}^{L_i} \ln \left\{ 1 - \left[1 - \exp \left(\frac{(i-d)}{(vV_{i-1})^{1/(d-i-1)}} \int_{(vV_{i-1})^{1/(d-i-1)}}^{(vV_{i-1})^{1/(d-i-1)} l} g_2(z^{d-i-1}) \right) \right]^{2l^{d-i} V_{i-1}} \right\}, \end{aligned} \quad (\text{C11})$$

where we changed the sum over k to an integral over $z = k (vV_{i-1})^{1/(d-i-1)}$. We now assume that the system is not strongly confined and that there are s small sides such that $(vV_{s-1})^{1/(d-s-1)} L_s \ll 1$ and $(vV_s)^{1/(d-s-2)} L_{s+1} \gg 1$. The equation for the critical density can then be further approximated by

$$\begin{aligned} 0 &= \ln V_d + (d-s) \sum_{l=1}^{L_{s+1}} \ln \left\{ 1 - \left[1 - \exp \left(\frac{(s+1-d)}{(vV_s)^{1/(d-s-2)}} \int_0^\infty g_2(z^{d-s-2}) dz \right) \right]^{2^{l^{d-s-1} V_s}} \right\} \\ 0 &= \ln V_d + (d-s) \sum_{l=1}^{L_{s+1}} \ln \left\{ 1 - \left[1 - \exp \left(\frac{\lambda_{d-s,3}(s+1-d)}{(vV_s)^{1/(d-s-2)}} \right) \right]^{2^{l^{d-s-1} V_s}} \right\} \\ &\approx \ln V_d + (d-s) \sum_{l=1}^{L_{s+1}} \ln \left\{ 1 - \exp \left[-2^{l^{d-s-1} V_s} \exp \left(\frac{\lambda_{d-s,3}(s+1-d)}{(vV_s)^{1/(d-s-2)}} \right) \right] \right\}. \end{aligned} \quad (\text{C12})$$

Changing the sum over l to an integral over $z = lV_s^{1/(d-s-1)}$ $\exp[-\lambda_{d-s,3}/(vV_s)^{1/(d-s-2)}]$ yields

$$\begin{aligned} 0 &= \ln V_d + \frac{(d-s) \exp[\lambda_{d-s,3}/(vV_s)^{1/(d-s-2)}]}{V_s^{1/(d-s-1)}} \\ &\times \int_0^\infty \ln \{ 1 - \exp[-2z^{d-s-1}] \} dz. \end{aligned} \quad (\text{C13})$$

Solving this equation yields

$$v_c \approx \frac{1}{V_s} \left(\frac{\lambda_{d-s,3}}{\ln \ln V_d} \right)^{d-s-2}. \quad (\text{C14})$$

If the two largest sides L_d and L_{d-1} are much larger than the other sides, i.e., $d_{\text{eff}} = 2$, the system is quasi-2D. In this case, since the expansion of the droplet in $m = 3$ requires at least three dimensions, the droplet can unblock only a finite region. Hence, the system is divided into clusters, each of which either contains a droplet or not. At the critical density we assume that the size of the frozen and unfrozen clusters is the same and equal to $\rho^{-4V_{d-2}}$, such that the critical density satisfies the equation

$$\begin{aligned} v_c &\approx \frac{1}{V_t} \left(\frac{\lambda_{d-t,3}}{\ln \ln (V_{d-2} \exp[8v_c V_{d-2}])} \right)^{d-t-2} \\ &\approx \frac{1}{V_t} \left(\frac{\lambda_{d-t,3}}{\ln 8v_c V_{d-2}} \right)^{d-t-2}. \end{aligned} \quad (\text{C15})$$

If there is one large side, $d_{\text{eff}} = 1$, the system behaves as a tunnel. Similarly to tunnels in three dimensions, the average section length is

$$\langle l \rangle = \exp \left\{ 2V_{d-1} \exp \left[-\frac{(d-t-1)\lambda_{d-t,3}}{(vV_t)^{1/(d-t-2)}} \right] \right\}, \quad (\text{C16})$$

and thus the critical density satisfies the equation

$$\begin{aligned} v_c &\approx \frac{1}{V_t} \left(\frac{\lambda_{d-t,3}}{\ln \ln (V_{d-1} \langle l \rangle)} \right)^{d-t-2} \\ \Rightarrow v_c &= \frac{1}{V_t} \left(\frac{(d-t)\lambda_{d-t,3}}{\ln [2V_{d-1}]} \right)^{d-t-2}, \end{aligned} \quad (\text{C17})$$

which is similar to that for a $(d-t-1)$ -dimensional system in the $m = 2$ model.

3. Critical density in general hyper-rhomboids

Since the full derivation of the critical density in $m > 3$ is very cumbersome, we provide here only a sketch, which is very similar to the derivation of the critical density in $m = 3$. Consider a hypercube in $d \geq m$ dimensions. This hypercube can be expanded if each of its sides has two hyperlayers of $d-1$ dimensions which can be emptied in a manner similar to a $m-1$ model. Now look at the $(d-2)$ -dimensional sides of these layers. They must be emptied in a manner similar to that in an $m-2$ model, etc. At the end, there is a $(d-m+2)$ -dimensional hypersurface which must be emptied as in an $m=2$ model. Each such iteration of surfaces of lower dimensions adds another exponent to the probability of a site belonging to a critical droplet, and therefore the critical density Eq. (1) depends on $m-1$ iterations of the \ln function. More specifically, we can write the probability of expanding a hypercube up to linear size L as

$$P_m = \prod_{l=1}^L f_{m-2,m}^d(l), \quad (\text{C18})$$

where $f_{n,m}(l)$ is defined by the recursion relation

$$\begin{aligned} f_{n+1,m}(l) &= 1 - \left(1 - \prod_{k=1}^l f_{n,m}(k) \right)^{(m-1)l^{d+n-1}}, \\ f_{0,m}(l) &= \beta_m(l) \\ &= \frac{1 - \rho^{(m-1)l} + \sqrt{(1 + \rho^{(m-1)l})^2 - 4\rho^{ml}}}{2}. \end{aligned} \quad (\text{C19})$$

Approximating P_m as was done before (changing the products to integrals of \ln functions, etc.) and solving the equation $1 = L^d P_m$ yields Eq. (1).

If the number of effective dimensions of the hyper-rhomboid is at least m , the system is either almost completely frozen or almost completely unfrozen and there is no division into sections or clusters. Assuming that there are s small sides, then in the integrals of g_{m-1} [as in Eqs. (C4) and (C11)] the upper limits of the first s integrals can be taken to zero and the lower limits of the last $d-s-1$ integrals can be taken to infinity, such that only one integral remains, which yields $\lambda_{d-s,m}/(vV_s)^{1/(d-s-m+1)}$. The other outer integrals yield unimportant constants (similarly to μ in the $m=3$ case), and each iteration of the f function gives another exponent, such

that in the end the critical density is

$$v_c = \frac{1}{V_s} \left(\frac{\lambda_{d-s,m}}{\ln_{(m-1)} V^{1/(d-s)}} \right)^{d-s-m+1}, \quad (\text{C20})$$

which is similar to the behavior of a $(d-s)$ -dimensional system.

If $d_{\text{eff}} < m$, the hyper-rhomboid is divided into clusters. If $d_{\text{eff}} = m - 1$, the characteristic size of the clusters is determined by the characteristic size of the clusters on the $d - 1$ dimensional hypersurfaces, which ultimately depends on the size of the subsection on the hypersurface unblocked via the $m = 2$ process, which is now a tunnel. The characteristic cluster size is thus $\rho^{-cV_{d-m+1}}$ in this case, where c is some constant which depends on d and m . If $d_{\text{eff}} = m - 2$, the characteristic size of the clusters is ultimately determined by the size of the subsections on the hypersurface (which is a tunnel) unblocked via the $m = 3$ process, which is $\sim \exp[V_{d-m+2} \exp(-2\lambda_{d,m}/v)]$. In general, the characteristic cluster size is determined by the size of the subsections on the hypersurface (which is a tunnel) unblocked via the $m - d_{\text{eff}} + 1$ process, which is $\sim \exp^{d_{\text{eff}}-1}[V_t \exp(-2\lambda_{d,m}/v)]$, with \exp^n being an exponential iterated n times. Due to the combination of the iterated \ln functions and the exponents, the critical vacancy density in all cases scales as

$$v_c \sim [\ln_{(m-2)} V_s^{1/(d-t)}]^{-d+t+m-1}, \quad (\text{C21})$$

which is similar to the result in a $(d-t-1)$ -dimensional system in an $m - 1$ model.

APPENDIX D: THE RELATION BETWEEN THE CORRELATION BETWEEN FROZEN SITES AND THE FLUCTUATIONS OF n_F

Consider the correlation between sites \vec{i} and \vec{j} ,

$$c_{\vec{i},\vec{j}} = \frac{1}{A} \sum_{\alpha} (n_i^{\alpha} - \rho n_F)(n_j^{\alpha} - \rho n_F), \quad (\text{D1})$$

where the sum is over all configurations α , the total number of configurations is A , for each site n_i^{α} is equal to 1 if the site contains a frozen particle in configuration α and is equal to zero in all other cases, and ρn_F is the average fraction of frozen sites,

$$\rho n_F = \frac{1}{AV} \sum_{\vec{i},\alpha} n_i^{\alpha}. \quad (\text{D2})$$

The average correlation is

$$C_{av} = \frac{1}{V^2} \sum_{\vec{i},\vec{j}} c_{\vec{i},\vec{j}}, \quad (\text{D3})$$

where V is the volume of the system. Using the definition of $c_{\vec{i},\vec{j}}$, Eq. (D1), in Eq. (D3) yields

$$\begin{aligned} C_{av} &= \frac{1}{AV^2} \sum_{\vec{i},\vec{j},\alpha} (n_i^{\alpha} - \rho n_F)(n_j^{\alpha} - \rho n_F) \\ &= \frac{1}{AV^2} \sum_{\vec{i},\vec{j},\alpha} [n_i^{\alpha} n_j^{\alpha} - n_i^{\alpha} \rho n_F - n_j^{\alpha} \rho n_F + \rho^2 n_F^2]. \end{aligned} \quad (\text{D4})$$

In the second term we sum over \vec{j} , in the third term we sum over \vec{i} , and in the fourth term we sum over \vec{i} , \vec{j} , and α , such that

$$\begin{aligned} C_{av} &= \frac{1}{AV^2} \sum_{\vec{i},\vec{j},\alpha} n_i^{\alpha} n_j^{\alpha} - \frac{1}{AV} \sum_{\vec{i},\alpha} n_i^{\alpha} \rho n_F \\ &\quad - \frac{1}{AV} \sum_{\vec{j},\alpha} n_j^{\alpha} \rho n_F + \rho^2 n_F^2. \end{aligned} \quad (\text{D5})$$

Using Eq. (D2) in the second and third terms yields

$$C_{av} = \frac{1}{AV^2} \sum_{\vec{i},\vec{j},\alpha} n_i^{\alpha} n_j^{\alpha} - \rho^2 n_F^2. \quad (\text{D6})$$

Now consider the fluctuations in ρn_F

$$\sigma^2 = \frac{1}{A} \sum_{\alpha} (\rho n_F^{\alpha})^2 - \rho^2 n_F^2, \quad (\text{D7})$$

where ρn_F^{α} is the fraction of frozen sites in configuration α ,

$$\rho n_F^{\alpha} = \frac{1}{V} \sum_{\vec{i}} n_i^{\alpha}. \quad (\text{D8})$$

Using Eq. (D8) in Eq. (D7) yields

$$\sigma^2 = \frac{1}{A} \sum_{\alpha} \left(\frac{1}{V} \sum_{\vec{i}} n_i^{\alpha} \right) \left(\frac{1}{V} \sum_{\vec{j}} n_j^{\alpha} \right) - \rho^2 n_F^2, \quad (\text{D9})$$

which is equal to Eq. (D6), and thus $\sigma^2 = C_{av}$.

Note that this result is valid in more general conditions: n_i^{α} can receive values other than zero or 1, the different configurations can have different weights, and the system can be continuous.

[1] A. J. Liu and S. R. Nagel, *Nature (London)* **396**, 21 (1998).
 [2] M. van Hecke, *J. Phys.: Condens. Matter* **22**, 033101 (2010).
 [3] A. J. Liu and S. R. Nagel, *Annu. Rev. Condens. Matter Phys.* **1**, 347 (2010).
 [4] G. Biroli and J. P. Garrahan, *J. Chem. Phys.* **138**, 12A301 (2013).
 [5] <http://www.rocksystems.com/machinery/conveyors>
 [6] http://www.slb.com/services/drilling/cementing/equipment/cement_slurry_defoamer.asp

[7] R. A. Bagnold, Geological Survey Professional Paper No. 422-I, I-20, 1966, <http://pubs.usgs.gov/pp/0422i/report.pdf>
 [8] <http://vulcan.wr.usgs.gov/Glossary/LavaTubes/framework.html>
 [9] D. J. Durian, *Phys. Rev. E* **55**, 1739 (1997).
 [10] T. K. Haxton and A. J. Liu, *Europhys. Lett.* **90**, 66004 (2010).
 [11] C. S. O'Hern, L. E. Silbert, A. J. Liu, and S. R. Nagel, *Phys. Rev. E* **68**, 011306 (2003).

- [12] N. Xu, V. Vitelli, M. Wyart, A. J. Liu, and S. R. Nagel, *Phys. Rev. Lett.* **102**, 038001 (2009).
- [13] E. Lerner, I. Procaccia, and J. Zylberg, *Phys. Rev. Lett.* **102**, 125701 (2009).
- [14] B. Andreotti, J.-L. Barrat, and C. Heussinger, *Phys. Rev. Lett.* **109**, 105901 (2012).
- [15] N. Saklayen, G. L. Hunter, K. V. Edmond, and E. R. Weeks, in *Fourth International Symposium on Slow Dynamics in Complex Systems*, edited by M. Tokuyama and I. Oppenheim, AIP Conf. Proc. No. 1518 (AIP, New York, 2013), p. 328.
- [16] A. I. Campbell and M. D. Haw, *Soft Matter* **6**, 4688 (2010).
- [17] K. N. Nordstrom, E. Verneuil, P. E. Arratia, A. Basu, Z. Zhang, A. G. Yodh, J. P. Gollub, and D. J. Durian, *Phys. Rev. Lett.* **105**, 175701 (2010).
- [18] M. A. Lohr, A. M. Alsayed, B. G. Chen, Z. Zhang, R. D. Kamien, and A. G. Yodh, *Phys. Rev. E* **81**, 040401(R) (2010).
- [19] K. E. Daniels and R. P. Behringer, *J. Stat. Mech.: Theory Exp.* (2006) P07018.
- [20] D. Bi, J. Zheng, B. Chakraborty, and R. P. Behringer, *Nature (London)* **480**, 355 (2011).
- [21] K. V. Edmond, C. R. Nugent, and E. R. Weeks, *Phys. Rev. E* **85**, 041401 (2012).
- [22] P. J. Yunker, K. Chen, Z. Zhang, and A. G. Yodh, *Phys. Rev. Lett.* **106**, 225503 (2011).
- [23] A. Ghosh, V. K. Chikkadi, P. Schall, J. Kurchan, and D. Bonn, *Phys. Rev. Lett.* **104**, 248305 (2010).
- [24] J. Cheng, J. H. McCoy, J. N. Israelachvili, and I. Cohen, *Science* **333**, 1276 (2011).
- [25] F. Ritort and P. Sollich, *Adv. Phys.* **52**, 219 (2003).
- [26] J. P. Garrahan, P. Sollich, and C. Toninelli, in *Dynamical Heterogeneities in Glasses, Colloids, and Granular Media*, edited by L. Berthier, G. Biroli, J.-P. Bouchaud, L. Cipelletti, and W. van Saarloos (Oxford University Press, New York, 2011), Chap. 10, [arXiv:1009.6113v1](https://arxiv.org/abs/1009.6113v1).
- [27] J. Jäckle and A. Krönig, *J. Phys.: Condens. Matter* **6**, 7633 (1994); A. Krönig and J. Jäckle, *ibid.* **6**, 7655 (1994).
- [28] S. M. Fielding, *Phys. Rev. E* **66**, 016103 (2002).
- [29] C. Toninelli, G. Biroli, and D. S. Fisher, *Phys. Rev. Lett.* **92**, 185504 (2004).
- [30] M. Sellitto, G. Biroli, and C. Toninelli, *Europhys. Lett.* **69**, 496 (2005).
- [31] C. Toninelli, G. Biroli, and D. S. Fisher, *Phys. Rev. Lett.* **96**, 035702 (2006).
- [32] F. Corberi and L. F. Cugliandolo, *J. Stat. Mech.: Theory Exp.* (2009) P09015.
- [33] A. Ghosh, E. Teomy, and Y. Shokef, [arXiv:1310.8273](https://arxiv.org/abs/1310.8273).
- [34] J. P. Garrahan, R. L. Jack, V. Lecomte, E. Pitard, K. van Duijvendijk, and F. van Wijland, *Phys. Rev. Lett.* **98**, 195702 (2007).
- [35] M. Sellitto, *Phys. Rev. Lett.* **101**, 048301 (2008).
- [36] M. Jeng and J. M. Schwarz, *Phys. Rev. E* **81**, 011134 (2010).
- [37] Y. Shokef and A. J. Liu, *Europhys. Lett.* **90**, 26005 (2010).
- [38] Y. S. Elmatad, R. L. Jack, D. Chandler, and J. P. Garrahan, *Proc. Natl. Acad. Sci. USA* **107**, 12793 (2010).
- [39] F. Turci and E. Pitard, *Fluct. Noise Lett.* **11**, 1242007 (2012).
- [40] F. Turci, E. Pitard, and M. Sellitto, *Phys. Rev. E* **86**, 031112 (2012).
- [41] J. Jackle and S. Eisinger, *Z. Phys. B* **84**, 115 (1991).
- [42] J. Reiter, F. Mauch, and J. Jackle, *Physica A* **184**, 458 (1992).
- [43] C. Kipnis, C. Marchioro, and E. Presutti, *J. Stat. Phys.* **27**, 65 (1980).
- [44] B. Derrida, *Phys. Rev. Lett.* **45**, 79 (1980).
- [45] B. Derrida, *Phys. Rev. B* **24**, 2613 (1981).
- [46] J.-P. Bouchaud, *J. Phys. I* **2**, 1705 (1992).
- [47] B. Derrida, M. R. Evans, and D. Mukamel, *J. Phys. A* **26**, 4911 (1993).
- [48] C. Monthus and J.-P. Bouchaud, *J. Phys. A* **29**, 3847 (1996).
- [49] Z. T. Nemeth and H. Lowen, *Phys. Rev. E* **59**, 6824 (1999).
- [50] P. Scheidler, W. Kob, and K. Binder, *Europhys. Lett.* **52**, 277 (2000).
- [51] F. Varnik, J. Baschnagel, and K. Binder, *Phys. Rev. E* **65**, 021507 (2002).
- [52] Y. Srebro and D. Levine, *Phys. Rev. Lett.* **93**, 240601 (2004).
- [53] M. R. Evans and T. Hanney, *J. Phys. A* **38**, R195 (2005).
- [54] S. Lang, V. Botan, M. Oettel, D. Hajnal, T. Franosch, and R. Schilling, *Phys. Rev. Lett.* **105**, 125701 (2010).
- [55] W. Kob and H. C. Andersen, *Phys. Rev. E* **48**, 4364 (1993).
- [56] G. H. Fredrickson and H. C. Andersen, *Phys. Rev. Lett.* **53**, 1244 (1984).
- [57] G. H. Fredrickson and H. C. Andersen, *J. Chem. Phys.* **83**, 5822 (1985).
- [58] J.-P. Bouchaud and G. Biroli, *J. Chem. Phys.* **121**, 7347 (2004).
- [59] L. Berthier and W. Kob, *Phys. Rev. E* **85**, 011102 (2012).
- [60] J. Balogh, B. Bollobas, H. Duminil-Copin, and R. Morris, *Trans. Am. Math. Soc.* **364**, 2667 (2012).
- [61] J. Gravner and A. E. Holroyd, *Ann. Appl. Probab.* **18**, 909 (2008).
- [62] E. Teomy and Y. Shokef, *Phys. Rev. E* **86**, 051133 (2012).
- [63] A. E. Holroyd, *Probab. Theory Relat. Fields* **125**, 194 (2003).
- [64] E. Teomy and Y. Shokef (unpublished).
- [65] <http://functions.wolfram.com/01.32.02.0001.01>
- [66] I. Einav, A. Dyskin, and B. Sukumaran, in *Geomechanics and Geotechnics of Particulate Media*, edited by M. Hyodo, H. Murata, and Y. Nakata (Taylor & Francis Group, London, 2006), pp. 157–160.
- [67] <http://functions.wolfram.com/03.04.07.0001.01>, after integration by parts.